Condensate pair fluctuations in a two-dimensional *d*-wave superconductor and Raman scattering

Wen-Chin Wu and A. Griffin
Department of Physics, University of Toronto, Toronto, Ontario, Canada M5S 1A7
(Received 3 August 1994)

The condensate pair fluctuations in the frequency region $\omega \lesssim 2\Delta$ and the associated Raman-scattering intensity of a two-dimensional (2D) d-wave weak-coupling BCS superconductor are investigated. Our model includes a dominant $d_{x^2-y^2}$ (L=2) and a weaker s-wave (L=0) pairing interaction. All response functions involving density and pair operators are evaluated (in the low-$\mathbf{q}$ limit). For neutral d-wave superconductors (no Coulomb interaction), the expected phononlike phase mode is obtained in the L=0 channel (which couples to density fluctuations). In contrast, excitonlike modes corresponding to excited Cooper pair states are obtained in the L=2 channel. We find an amplitude fluctuation mode with frequency $\sqrt{3}\Delta$. For charged d-wave superconductors, the L=0 phonon is renormalized into a 2D plasmon, but the L=2 excitonlike mode remains unaffected by the Coulomb interaction. At T=0, the latter is shown to be completely washed out in the Raman scattering spectrum ($\mathbf{q}=0$) due to large p-h damping (which arises in the absence of a finite pair breaking gap in d-wave superconductors). However, at finite temperatures, we find the energy of the excitonlike mode is drastically lowered [relative to $2\Delta(T)$] when the s-wave attraction is comparable to the d-wave pairing. This leads to a decrease in the damping and, as a result, the mode shows up as a low-frequency resonance in the Raman cross section. Due to the anisotropy of the d-wave order parameter, the quasiparticle excitation spectrum and the noninteracting two-particle spectrum are strongly dependent on the direction of $\mathbf{q}$. We also find that the excitonlike mode frequency becomes anisotropic for wave vectors of the order of Δ/v_F.

I. INTRODUCTION

Recently d-wave pairing in the high-T_c layered superconductors has been of increasing interest in both theoretical[1–4] and experimental[5–8] studies (further references are given in these papers), although unambiguous evidence for d-wave pairing is still missing. d-wave superconductors involve an order parameter describing a Cooper pair condensate which is anisotropic, with nodes at various points on the Fermi surface. As a result, the frequency and spectral weight of the BCS quasiparticles are strongly dependent on the direction of the propagation wave vector $\mathbf{q}$. This in turn modifies the properties of the collective modes. In view of the potential relevance in layered high-T_c copper oxides, we present a detailed analysis of the collective modes associated with Cooper pair fluctuations in two-dimensional (2D) d-wave superconductors. Our work is easily generalized to three-dimensional (3D) layered d-wave superconductors if we ignore electronic tunneling between layers, as done for s-wave superconductors in Ref. 9.

Hirashima and Namaizawa[10] have made a detailed study of the collective modes for 3D d-wave superconductors, including different order parameter symmetries and the effect of the Coulomb interaction. However, they did not discuss excitonlike modes or consider the effect of strong damping. Recent work of Devereaux *et al.*[11] has given a detailed analysis of the effect of vertex corrections (and the resulting collective modes) on Raman scattering in 3D and 2D superconductors, but only considered pairing in the d-wave channel. In our work, we discuss the collective mode spectrum at finite $\mathbf{q}$, as well as at $\mathbf{q}=0$ which is probed by Raman scattering. We emphasize the role of a strong s-wave attractive interaction on the collective mode spectrum of a d-wave superconductor. In Raman scattering, we show that while the resonances from excitonlike modes are washed out at low T, they may show up at temperatures close to T_c if the s-wave pairing interaction is appreciable. In general, our results show characteristic differences from predictions based on considering only two noninteracting quasiparticles (i.e., when vertex corrections are ignored).

In contrast with previous work, which dealt with 3D d-wave superconductors,[10,11] we consider a 2D superconductor. As is well known, a major feature of a 2D superconductor is that plasmons have low energies at long wavelengths, with an energy less than 2Δ.[9]

The particle-particle (pairing) interaction can be decomposed into various symmetries using[12,13]

$$g(\mathbf{p}-\mathbf{p}') = \sum_L g_L f_L(\hat{\mathbf{p}}) f_L^*(\hat{\mathbf{p}}'), \tag{1}$$

where, in 2D, L represents the azimuthal angular momentum m. The orthonormal angle functions $f_L(\hat{\mathbf{q}})$ are defined on the Fermi surface (assumed to be circular in 2D) and the pairing interaction is rotationally invariant. We assume that the most important contributions to the pairing interaction are s- and $d_{x^2-y^2}$-wave components in a spin-singlet state, i.e.,

$$g(\mathbf{p}-\mathbf{p}') = g_{L=0} f_{L=0}(\hat{\mathbf{p}}) f_{L=0}(\hat{\mathbf{p}}') + g_{L=2} f_{L=2}(\hat{\mathbf{p}}) f_{L=2}(\hat{\mathbf{p}}'), \qquad (2)$$

where $f_{L=0}(\hat{\mathbf{p}}) \equiv 1$ and $f_{L=2}(\hat{\mathbf{p}}) \equiv \sqrt{2}\cos(2\phi')$ (ϕ' is the angle of $\mathbf{p}$ on the Fermi surface). With this model pairing interaction, one can discuss both *s*- and *d*-wave superconductors. In this paper, we limit ourselves to pure spin-singlet pairing and exclude the possibility of spin fluctuations arising from spin-triplet states.

The well known self-consistent weak-coupling BCS gap equation which $\Delta_{\mathbf{p}}(T)$ satisfies is given by

$$\Delta_{\mathbf{p}}(T) = -\int \frac{d\mathbf{p}'}{(2\pi)^2} g(\mathbf{p}-\mathbf{p}') \frac{\Delta_{\mathbf{p}'}(T)}{2E_{\mathbf{p}'}}[1 - 2n_F(E_{\mathbf{p}'})], \qquad (3)$$

where $n_F(E) = [\exp(\beta E)+1]^{-1}$ is the Fermi function with $\beta = (k_B T)^{-1}$. If $g_{L=0}$ dominates, superconductivity of *s*-wave type is the most stable. In this case, the solution of (3) is found to be isotropic, i.e., $\Delta_{\mathbf{p}}(T) = \Delta(T)$. If $g_{L=2}$ dominates, *d*-wave superconductivity arises, with a *d*-wave order parameter which is anisotropic. In this case, the solution of (3) is of the form $\Delta_{\mathbf{p}}(T) = \Delta(T) f(\hat{\mathbf{p}})$, with $f(\hat{\mathbf{p}}) = f_{L=2}(\hat{\mathbf{p}})/\sqrt{2} = \cos(2\phi')$.[14] This *d*-wave order parameter looks like a four-leaf clover with four nodes on the Fermi surface (see Fig. 1) and corresponds to the continuum limit of the well known tight-binding expression

$$\Delta_{\mathbf{p}}(T) = \Delta(T)[\cos(p_x a) - \cos(p_y a)] , \qquad (4)$$

discussed in the recent literature.[1–4] In this paper, for simplicity, we exclude the possibility of a solution of (3) which is a mixture of *s*- and *d*-wave components, which can arise due to the highly nonlinear nature of (3).

In conventional isotropic *s*-wave superconductors, the Cooper pair collective modes are well known: the (phase) Anderson-Bogoliubov (AB) phonon mode which arises in neutral superconductors and couples into the density fluctuations,[9,12,15–18] and an amplitude mode[19] which appears close to the isotropic pair breaking energy 2Δ and is decoupled from the density fluctuations. As a

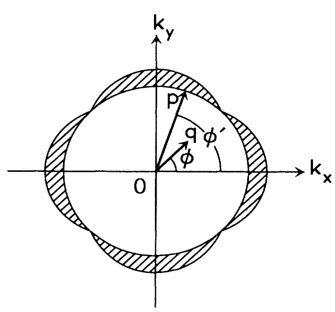

FIG. 1. Sketch of the *magnitude* of the order parameter (hatched area) for a 2D *d*-wave superconductor, where ϕ is the angle between the momentum $\mathbf{q}$ and the $\mathbf{k}_x$ axis and ϕ' is the angle between the quasiparticle momentum $\mathbf{p}$ and the $\mathbf{k}_x$ axis.

result, the AB phonon mode is renormalized into a plasmon mode in charged superconductors, while the amplitude mode remains unaffected by the Coulomb interaction. Moreover, when an $L = 0$ channel Cooper pair is broken up into two quasiparticles, the so-called "residual pairing interaction" g_2 will cause them to form (excited-state) bound pairs which are orthogonal to the $L=0$ Cooper pairs. These are the well known $L=2$ excitonlike modes[12,20,21] which are also unaffected by the Coulomb interaction in the $\mathbf{q} \to 0$ limit. This is because in this limit the anisotropic $L=2$ modes involve no net contribution to the overall density fluctuation in *s*-wave superconductors.

In contrast, in *d*-wave superconductors, Cooper pairs are formed by the dominant pairing interaction g_2 and have $L=2$ symmetry. However, we show that while the phonon modes correspond to overall phase fluctuations of the *d*-wave order parameter ($L=2$), they are coupled into density fluctuations and therefore are shifted to the $L = 0$ channel. The long-range Coulomb interaction will thus renormalize the phonon into a plasmon in charged *d*-wave superconductors, a feature expected in any BCS-type superconductor, whatever the nature of the pairing. Analogous to the appearance of $L=2$ excitonlike modes in *s*-wave superconductors, the weaker "residual pairing interaction" g_0 may result in excited bound pairs. However, we show this leads to an excitonlike collective mode in the $L=2$ channel, which is unaffected by the Coulomb interaction.

As pair breaking can only arise at energies of 2Δ or greater for *s*-wave superconductors, collective modes are well defined for energies below 2Δ, but are damped for energies above 2Δ. In *d*-wave superconductors, in contrast, pair breaking can arise below as well as above 2Δ. In particular, collective modes at $\mathbf{q} = 0$ are always damped. However, when $\mathbf{q}$ is finite, the minimum energy $E_{\mathbf{p}} + E_{\mathbf{p}+\mathbf{q}}$ (at $T=0$) required to break up a Cooper pair and the spectral weight of the noninteracting two-particle spectrum are strongly dependent on the direction of $\mathbf{q}$. When this minimum is finite in a certain direction, a collective mode with a frequency smaller than this minimum energy can still be well defined (undamped). This anisotropy is obviously of great experimental interest in trying to obtain information about the symmetry of the order parameter in the cuprates. Moreover, the temperature plays a role in deciding whether a collective mode is strongly or only slightly damped. We find that the excitonlike modes become less damped at higher temperatures (this effect is maximum at $T \simeq 0.75T_c$) if g_0 is comparable to g_2. The reason for this somewhat surprising result is that as the temperature increases, the mode energy is lowered [relative to $2\Delta(T)$] into a region where the *p*-*h* decay channel is less effective.

When the pairing interaction is described by (2), one can show that there are four collective degrees of freedom for fluctuations of the complex order parameter, in addition to the density fluctuations. This gives rise to four branches of the collective mode spectrum. In the low-$\mathbf{q}$ limit, in *s*-wave superconductors, the $L = 0$ channel which projects out the $f_{L=0}(\hat{\mathbf{p}})$ contribution is decoupled from the $L=2$ channel, which projects out the

$f_{L=2}(\hat{\mathbf{p}})$ contribution. In contrast, we show that for d-wave superconductors, the L=0 and L=2 contributions couple together and lead to renormalized L=0 and L=2 channels. In this low-$\mathbf{q}$ limit, the collective modes corresponding to different renormalized channels can be studied. Although we have only included two channels in (2) for the pairing interaction, this is sufficient to bring out the essential physics and is of most physical interest in connection with the cuprates. The extension including other symmetries (channels) is straightforward.

In Sec. II, we derive the formalism for the analysis of the collective fluctuations and various density-density, density-pair, and pair-pair response functions. In Sec. III, we study 2D d-wave superconductors and work out the collective mode energy and damping in some detail at small but finite $\mathbf{q}$. In Sec. IV, we derive the cross section for Raman scattering including the collective fluctuations and evaluate it at both zero and finite temperatures. In Sec. V, we summarize our main conclusions and their relevance to Raman experimental studies on the cuprates. For the convenience of the reader, we briefly review analogous results for collective modes and the associated Raman-scattering intensities in s-wave superconductors in Appendix C.

II. RESPONSE FUNCTIONS

Our evaluation of the various response functions will be based on what is called the time-dependent Hartree-Fock approximation, generalized to superconductors. Calculating the response to the self-consistent Hartree field due to the Coulomb interaction corresponds to summing up polarization bubble diagrams [random phase approximation (RPA)]. Similarly, including the response to the self-consistent exchange fields due to the pairing interactions corresponds to summing up the ladders in the bubble diagrams (ladder approximation for the vertex functions). An alternative Green's function derivation of these response functions could begin with the generalized RPA (GRPA) equations of motion in conjunction with (2), as summarized by Eqs. (4.5) and (4.6) of Côté and Griffin[9] (hereafter referred to as CG). We believe the linear response analysis[22] of this section is simpler and brings out the physics more clearly.

The total Hamiltonian $K = H - \mu N$ of the interacting electron gas can be described by

$$K = \sum_{\mathbf{p},\sigma} \epsilon_{\mathbf{p}} a^{\dagger}_{\mathbf{p},\sigma} a_{\mathbf{p},\sigma} + \frac{1}{2} \sum_{\mathbf{p},\mathbf{p}',\mathbf{q},\sigma,\sigma'} V(\mathbf{q}) a^{\dagger}_{\mathbf{p}+\mathbf{q},\sigma} a^{\dagger}_{\mathbf{p}'-\mathbf{q},\sigma'} a_{\mathbf{p}',\sigma'} a_{\mathbf{p},\sigma}, \tag{5}$$

where $a_{\mathbf{p},\sigma}$, $a^{\dagger}_{\mathbf{p},\sigma}$ are the usual destruction and creation operators for electrons and the kinetic energy with respect to the Fermi energy is $\epsilon_{\mathbf{p}} = \mathbf{p}^2/2m - \mu$. The two-particle interaction V_2 given by the second term on the right-hand side (rhs) of (5) can be approximated in the BCS superconducting state using the time-dependent Hartree-Fock-Gor'kov mean-field approximation (MFA) for a perturbed system,

$$V_2 \equiv \frac{1}{2} \sum_{\mathbf{p},\mathbf{p}',\mathbf{q},\sigma} \Bigg[2V(\mathbf{q}) \langle a^{\dagger}_{\mathbf{p}+\mathbf{q},\sigma} a_{\mathbf{p},\sigma} \rangle \sum_{\sigma'} a^{\dagger}_{\mathbf{p}'-\mathbf{q},\sigma'} a_{\mathbf{p}',\sigma'} - 2V(\mathbf{p}-\mathbf{p}') \langle a^{\dagger}_{\mathbf{p},\sigma} a_{\mathbf{p}+\mathbf{q},\sigma} \rangle a^{\dagger}_{\mathbf{p}'+\mathbf{q},\sigma} a_{\mathbf{p}',\sigma}$$
$$+ V(\mathbf{p}-\mathbf{p}') \langle a^{\dagger}_{\mathbf{p},\sigma} a^{\dagger}_{-\mathbf{p}+\mathbf{q},-\sigma} \rangle a_{-\mathbf{p}'+\mathbf{q},-\sigma} a_{\mathbf{p}',\sigma} + V(\mathbf{p}-\mathbf{p}') \langle a_{-\mathbf{p}+\mathbf{q},-\sigma} a_{\mathbf{p},\sigma} \rangle a^{\dagger}_{\mathbf{p}',\sigma} a^{\dagger}_{-\mathbf{p}'+\mathbf{q},-\sigma} \Bigg], \tag{6}$$

where $\langle \hat{A} \rangle$ is determined self-consistently by the MFA Hamiltonian in (6). The first term on the rhs of (6) corresponds to the Hartree (direct) contribution. The other terms correspond to exchange contributions. In our case, we are dealing with the Coulomb interaction v and a pairing interaction g. We only include the long-range Coulomb interaction in the *Hartree* term in (6), which corresponds to the well-known random phase approximation when used to calculate response functions. In contrast, we only consider the short-range pairing interaction in the exchange or *Fock* terms in (6), which corresponds to the so-called generalized random phase approximation (see Ref. 9 for further discussion).

It is useful to define the following L-dependent density and pair order parameter operators:[20,21]

$$\begin{aligned}
\tilde{\rho}^{L}_{\mathbf{q}}(t) &= \frac{1}{\sqrt{2}} \sum_{\mathbf{p},\sigma} f_L(\hat{\mathbf{p}}) a^{\dagger}_{\mathbf{p},\sigma}(t) a_{\mathbf{p}+\mathbf{q},\sigma}(t), \\
\tilde{m}^{L}_{\mathbf{q},\sigma}(t) &= \sum_{\mathbf{p}} f_L(\hat{\mathbf{p}}) a_{-\mathbf{p}+\mathbf{q},-\sigma}(t) a_{\mathbf{p},\sigma}(t), \\
\tilde{m}^{\dagger,L}_{\mathbf{q},\sigma}(t) &= \sum_{\mathbf{p}} f^{*}_L(\hat{\mathbf{p}}) a^{\dagger}_{\mathbf{p},\sigma}(t) a^{\dagger}_{-\mathbf{p}-\mathbf{q},-\sigma}(t).
\end{aligned} \tag{7}$$

We note that in a d-wave superconductor, it is $\tilde{m}^{L=2}$ (and $\tilde{m}^{\dagger,L=2}$) which corresponds to the BCS order parameter. Making use of the model pairing interaction in (2), the mean-field approximation (6) for the effect of the two-particle interactions can be expressed in terms of the operators defined in (7) [note $f_0(\hat{\mathbf{p}}) \equiv 1$],

$$V_2 \equiv \sum_{\mathbf{q}} \left[2v_{\mathbf{q}} \langle \tilde{\rho}_{\mathbf{q}}^{L=0} \rangle \tilde{\rho}_{\mathbf{q}}^{\dagger,L=0} - \sum_L g_L \left(\langle \tilde{\rho}_{\mathbf{q}}^{L} \rangle \tilde{\rho}_{\mathbf{q}}^{\dagger,L} - \langle \tilde{m}_{\mathbf{q},\sigma}^{\dagger,L} \rangle \tilde{m}_{\mathbf{q},\sigma}^{L} - \langle \tilde{m}_{\mathbf{q},\sigma}^{L} \rangle \tilde{m}_{\mathbf{q},\sigma}^{\dagger,L} \right) \right], \tag{8}$$

where L=0,2 and we assume that the spin up ($\sigma=\uparrow$) and spin down ($\sigma=\downarrow$) give the same contribution. Here $v_{\mathbf{q}} = 2\pi e^2/q$ is the 2D Coulomb interaction. Following the literature,[20] the strength g_L here is assumed to be the same in both the Cooper (particle-particle) channel and the zero-sound (particle-hole) channels.

A perturbing Hamiltonian V_1 can be conveniently expressed in terms of $\tilde{\rho}_{\mathbf{q}}^{L}$, $\tilde{m}_{\mathbf{q},\sigma}^{L}$, and $\tilde{m}_{\mathbf{q},\sigma}^{\dagger,L}$,

$$V_1 = \sum_L \int \frac{d\mathbf{q}}{(2\pi)^2} [\delta\phi_L(\mathbf{q},\omega)\tilde{\rho}_{\mathbf{q}}^{L} + \delta\eta_L(\mathbf{q},\omega)\tilde{m}_{\mathbf{q},\sigma}^{\dagger,L} + \delta\eta_L^*(\mathbf{q},\omega)\tilde{m}_{\mathbf{q},\sigma}^{L}], \tag{9}$$

where the applied external perturbation $\delta\phi_L$ couples into the density $\tilde{\rho}_{\mathbf{q}}^{L}$ and the symmetry-breaking field $\delta\eta_L$ couples into $\tilde{m}_{\mathbf{q},\sigma}^{\dagger,L}$ and $\delta\eta_L^*$ couples into $\tilde{m}_{\mathbf{q},\sigma}^{L}$. Using linear response theory to calculate the effect of V_1 in (9), in conjunction with a mean-field approximation for the two-particle interaction in (8) appropriate to a superconductor, we obtain[22]

$$\begin{aligned}
\delta\tilde{\rho}^{L} &= \sum_{L'} \left[\chi_{\tilde{\rho}^L\tilde{\rho}^{L'}} \delta\phi_{L'} + \chi_{\tilde{\rho}^L\tilde{m}^{\dagger,L'}} \delta\eta_{L'} + \chi_{\tilde{\rho}^L\tilde{m}^{L'}} \delta\eta_{L'}^* \right] \\
&\equiv \sum_{L'} \left[\chi^0_{\tilde{\rho}^L\tilde{\rho}^{L'}} \delta\phi_{L',\text{eff}} + \chi^0_{\tilde{\rho}^L\tilde{m}^{\dagger,L'}} \delta\eta_{L',\text{eff}} + \chi^0_{\tilde{\rho}^L\tilde{m}^{L'}} \delta\eta_{L',\text{eff}}^* \right] \\
&\simeq \sum_{L'} \left[\chi^0_{\tilde{\rho}^L\tilde{\rho}^{L'}} [\delta\phi_{L'} - (g_{L'} - 2v_{\mathbf{q}}\delta_{L',0})\delta\tilde{\rho}^{L'}] + \chi^0_{\tilde{\rho}^L\tilde{m}^{\dagger,L'}} (\delta\eta_{L'} + g_{L'}\delta\tilde{m}^{L'}) + \chi^0_{\tilde{\rho}^L\tilde{m}^{L'}} (\delta\eta_{L'}^* + g_{L'}\delta\tilde{m}^{\dagger,L'}) \right],
\end{aligned} \tag{10}$$

where the various correlation functions in (10) are defined in terms of the L-dependent operators in (7),

$$\chi_{A^L B^{L'}}(\mathbf{q}, i\Omega_n) = -\int_0^\beta d\tau e^{i\Omega_n\tau} \langle \hat{\mathrm{T}}_\tau A_{\mathbf{q}}^L(\tau) B_{\mathbf{q}}^{\dagger,L'}(0) \rangle, \tag{11}$$

for $A,B = \tilde{\rho}, \tilde{m}, \tilde{m}^\dagger$ and $L,L' = 0,2$. Here we drop the spin label σ in $\tilde{m}^L$ and $\tilde{m}^{\dagger,L}$ for simplicity. The last line of (10) is written in terms of three self-consistent effective potentials $\delta\phi_{L,\text{eff}}$, $\delta\eta_{L,\text{eff}}$, and $\delta\eta_{L,\text{eff}}^*$ which arise from the "mean-field" approximation (8) to the various terms of the two-particle interaction. Within the same framework, we can write down the analogous linear response equations for $\tilde{m}^{\dagger,L}$ and $\tilde{m}^L$,

$$\begin{aligned}
\delta\tilde{m}^{\dagger,L} &= \sum_{L'} \left[\chi_{\tilde{m}^{\dagger,L}\tilde{\rho}^{L'}} \delta\phi_{L'} + \chi_{\tilde{m}^{\dagger,L}\tilde{m}^{\dagger,L'}} \delta\eta_{L'} + \chi_{\tilde{m}^{\dagger,L}\tilde{m}^{L'}} \delta\eta_{L'}^* \right] \\
&\equiv \sum_{L'} \left[\chi^0_{\tilde{m}^{\dagger,L}\tilde{\rho}^{L'}} \delta\phi_{L',\text{eff}} + \chi^0_{\tilde{m}^{\dagger,L}\tilde{m}^{\dagger,L'}} \delta\eta_{L',\text{eff}} + \chi^0_{\tilde{m}^{\dagger,L}\tilde{m}^{L'}} \delta\eta_{L',\text{eff}}^* \right] \\
&\simeq \sum_{L'} \left[\chi^0_{\tilde{m}^{\dagger,L}\tilde{\rho}^{L'}} [\delta\phi_{L'} - (g_{L'} - 2v_{\mathbf{q}}\delta_{L',0})\delta\tilde{\rho}^{L'}] + \chi^0_{\tilde{m}^{\dagger,L}\tilde{m}^{\dagger,L'}} (\delta\eta_{L'} + g_{L'}\delta\tilde{m}^{L'}) + \chi^0_{\tilde{m}^{\dagger,L}\tilde{m}^{L'}} (\delta\eta_{L'}^* + g_{L'}\delta\tilde{m}^{\dagger,L'}) \right]
\end{aligned} \tag{12}$$

and

$$\begin{aligned}
\delta\tilde{m}^{L} &= \sum_{L'} \left[\chi_{\tilde{m}^{L}\tilde{\rho}^{L'}} \delta\phi_{L'} + \chi_{\tilde{m}^{L}\tilde{m}^{\dagger,L'}} \delta\eta_{L'} + \chi_{\tilde{m}^{L}\tilde{m}^{L'}} \delta\eta_{L'}^* \right] \\
&\equiv \sum_{L'} \left[\chi^0_{\tilde{m}^{L}\tilde{\rho}^{L'}} \delta\phi_{L',\text{eff}} + \chi^0_{\tilde{m}^{L}\tilde{m}^{\dagger,L'}} \delta\eta_{L',\text{eff}} + \chi^0_{\tilde{m}^{L}\tilde{m}^{L'}} \delta\eta_{L',\text{eff}}^* \right] \\
&\simeq \sum_{L'} \left[\chi^0_{\tilde{m}^{L}\tilde{\rho}^{L'}} [\delta\phi_{L'} - (g_{L'} - 2v_{\mathbf{q}}\delta_{L',0})\delta\tilde{\rho}^{L'}] + \chi^0_{\tilde{m}^{L}\tilde{m}^{\dagger,L'}} (\delta\eta_{L'} + g_{L'}\delta\tilde{m}^{L'}) + \chi^0_{\tilde{m}^{L}\tilde{m}^{L'}} (\delta\eta_{L'}^* + g_{L'}\delta\tilde{m}^{\dagger,L'}) \right].
\end{aligned} \tag{13}$$

Since L and L' can be 0 or 2, one has to solve a 6×6 RPA-like matrix equation incorporating the above coupled equations (10), (12), and (13),

$$\begin{aligned}
\chi &= \chi^0 - \chi^0 V \chi \\
&= (\mathcal{I} + \chi^0 V)^{-1} \chi^0,
\end{aligned} \tag{14}$$

where $\mathcal{I}$ is the 6×6 unit matrix and χ is defined by

$$\chi = \begin{pmatrix} \chi_{\tilde\rho^0\tilde\rho^0} & \chi_{\tilde\rho^0\tilde\rho^2} & \chi_{\tilde\rho^0\tilde m^{\dagger,0}} & \chi_{\tilde\rho^0\tilde m^{\dagger,2}} & \chi_{\tilde\rho^0\tilde m^0} & \chi_{\tilde\rho^0\tilde m^2} \\ \chi_{\tilde\rho^2\tilde\rho^0} & \chi_{\tilde\rho^2\tilde\rho^2} & \chi_{\tilde\rho^2\tilde m^{\dagger,0}} & \chi_{\tilde\rho^2\tilde m^{\dagger,2}} & \chi_{\tilde\rho^2\tilde m^0} & \chi_{\tilde\rho^2\tilde m^2} \\ \chi_{\tilde m^{\dagger,0}\tilde\rho^0} & \chi_{\tilde m^{\dagger,0}\tilde\rho^2} & \chi_{\tilde m^{\dagger,0}\tilde m^{\dagger,0}} & \chi_{\tilde m^{\dagger,0}\tilde m^{\dagger,2}} & \chi_{\tilde m^{\dagger,0}\tilde m^0} & \chi_{\tilde m^{\dagger,0}\tilde m^2} \\ \chi_{\tilde m^{\dagger,2}\tilde\rho^0} & \chi_{\tilde m^{\dagger,2}\tilde\rho^2} & \chi_{\tilde m^{\dagger,2}\tilde m^{\dagger,0}} & \chi_{\tilde m^{\dagger,2}\tilde m^{\dagger,2}} & \chi_{\tilde m^{\dagger,2}\tilde m^0} & \chi_{\tilde m^{\dagger,2}\tilde m^2} \\ \chi_{\tilde m^0\tilde\rho^0} & \chi_{\tilde m^0\tilde\rho^2} & \chi_{\tilde m^0\tilde m^{\dagger,0}} & \chi_{\tilde m^0\tilde m^{\dagger,2}} & \chi_{\tilde m^0\tilde m^0} & \chi_{\tilde m^0\tilde m^2} \\ \chi_{\tilde m^2\tilde\rho^0} & \chi_{\tilde m^2\tilde\rho^2} & \chi_{\tilde m^2\tilde m^{\dagger,0}} & \chi_{\tilde m^2\tilde m^{\dagger,2}} & \chi_{\tilde m^2\tilde m^0} & \chi_{\tilde m^2\tilde m^2} \end{pmatrix} . \tag{15}$$

The interaction matrix in (14) is

$$V = \begin{pmatrix} g_0 - 2v_{\mathbf{q}} & 0 & 0 & 0 & 0 & 0 \\ 0 & g_2 & 0 & 0 & 0 & 0 \\ 0 & 0 & 0 & 0 & -g_0 & 0 \\ 0 & 0 & 0 & 0 & 0 & -g_2 \\ 0 & 0 & -g_0 & 0 & 0 & 0 \\ 0 & 0 & 0 & -g_2 & 0 & 0 \end{pmatrix} . \tag{16}$$

The general structure of (14) shows that the *complete* collective mode spectrum of the system will be given by the zeros of the secular determinant, i.e.,

$$\det(\mathcal{I} + \chi^0 V) = 0. \tag{17}$$

To a good approximation in the long-wavelength limit ($qv_F \ll \Delta$ or $q \ll \xi^{-1}$, where ξ is the BCS coherence length), the dominant matrix elements for various noninteracting correlation functions in (15) are found to be given by

$$\chi^0 = \begin{pmatrix} (a_0 - b_0) & 0 & 0 & \sqrt{2}c_1 & 0 & -\sqrt{2}c_1 \\ 0 & (a_2 - b_2) & \sqrt{2}c_1 & 0 & -\sqrt{2}c_1 & 0 \\ 0 & -\sqrt{2}c_1 & b_0 & 0 & -d_0 & 0 \\ -\sqrt{2}c_1 & 0 & 0 & b_2 & 0 & -d_2 \\ 0 & \sqrt{2}c_1 & -d_0 & 0 & b_0 & 0 \\ \sqrt{2}c_1 & 0 & 0 & -d_2 & 0 & b_2 \end{pmatrix} , \tag{18}$$

where explicit expressions for the functions a_ℓ, b_ℓ, c_ℓ, and d_ℓ (ℓ=0,1,2) are defined in Appendix A for T=0. Using (16)–(18), we obtain

$$\det(\mathcal{I} + \chi^0 V) = D_0 D_2 D_0' D_2', \tag{19}$$

where we have introduced the four new functions

$$D_0 \equiv [1 + (g_0 - 2v_{\mathbf{q}})A_0](1 + g_2 B_2) + 4(g_0 - 2v_{\mathbf{q}})g_2 c_1^2, \tag{20}$$

$$D_2 \equiv (1 + g_2 A_2)(1 + g_0 B_0) + 4 g_0 g_2 c_1^2, \tag{21}$$

$$D_\ell' \equiv 1 + g_\ell(d_\ell - b_\ell) \qquad (\ell = 0, 2), \tag{22}$$

with $A_\ell \equiv a_\ell - b_\ell$ and $B_\ell \equiv b_\ell + d_\ell$ (ℓ=0,2), as in CG. One can see from (19)–(22) that, in principle, there are four kinds of collective modes in a 2D d-wave superconductor. Two branches are given by $\mathrm{Re}D_\ell = 0$ and another two are given by $\mathrm{Re}D_\ell' = 0$ (ℓ=0,2). The long-range Coulomb interaction is seen to only renormalize the collective mode given by $\mathrm{Re}D_0 = 0$. It has no effect on the other modes, at least in the long-wavelength limit we are considering.

Of these four possible collective mode branches, we shall see in Sec. III that the zeros of $\mathrm{Re}D_0$ correspond to the collective modes appearing in the L=0 channel (they appear in the isotropic density response function). In contrast, the zeros of $\mathrm{Re}D_2$ correspond to the collective modes in the L=2 channel. More explicitly, the solution of $\mathrm{Re}D_0 = 0$ corresponds to phase modes associated with the d-wave order parameter fluctuations, while $\mathrm{Re}D_2 = 0$ gives excitonlike modes. Due to the phase fluctuations coupling into the density fluctuations, the phase modes are strongly renormalized by the long-range Coulomb interaction, as can be seen in (20). In contrast, the excitonlike modes correspond to the excited Cooper pair states which remain unaffected by Coulomb interaction. The solutions of $\mathrm{Re}D_\ell' = 0$ (ℓ=0,2) correspond to amplitude modes of the d-wave order parameter and are not affected by the Coulomb interaction, as shown explicitly by (22).

Solving the RPA-like matrix equation in (14) (using MAPLE software), we obtain explicit expressions for all the nonvanishing correlation functions in the 6×6 matrix (15):

$$\chi_{\tilde\rho^0\tilde\rho^0} = \frac{A_0(1 + g_2 B_2) + 4 g_2 c_1^2}{D_0} \equiv \chi_{\rho\rho}, \tag{23}$$

$$\chi_{\tilde\rho^2\tilde\rho^2} = \frac{A_2(1 + g_0 B_0) + 4 g_0 c_1^2}{D_2}, \tag{24}$$

$$\chi_{\tilde\rho^0\tilde m^{\dagger,2}} = \chi_{\tilde m^2\tilde\rho^0} = -\chi_{\tilde\rho^0\tilde m^2} = -\chi_{\tilde m^{\dagger,2}\tilde\rho^0} = \frac{\sqrt{2}c_1}{D_0}, \tag{25}$$

$$\chi_{\tilde{\rho}^2 \tilde{m}^{\dagger,0}} = \chi_{\tilde{m}^0 \tilde{\rho}^2} = -\chi_{\tilde{\rho}^2 \tilde{m}^0} = -\chi_{\tilde{m}^{\dagger,0} \tilde{\rho}^2} = \frac{\sqrt{2} c_1}{D_2}, \tag{26}$$

$$\chi_{\tilde{m}^{\dagger,0} \tilde{m}^{\dagger,0}} = \chi_{\tilde{m}^0 \tilde{m}^0} = \frac{b_0(1 + g_2 A_2) + 2 g_2 c_1^2}{D_2 D_0'}, \tag{27}$$

$$\chi_{\tilde{m}^{\dagger,0} \tilde{m}^0} = \chi_{\tilde{m}^0 \tilde{m}^{\dagger,0}} = \frac{(1 + g_2 A_2)(g_0 b_0^2 - g_0 d_0^2 - d_0) + 2 g_2 c_1^2 [2 g_0 (b_0 - d_0) - 1]}{D_2 D_0'}, \tag{28}$$

$$\chi_{\tilde{m}^{\dagger,2} \tilde{m}^{\dagger,2}} = \chi_{\tilde{m}^2 \tilde{m}^2} = \frac{b_2[1 + (g_0 - 2v_{\mathbf{q}})A_0] + 2(g_0 - 2v_{\mathbf{q}}) c_1^2}{D_0 D_2'}, \tag{29}$$

$$\begin{aligned} \chi_{\tilde{m}^{\dagger,2} \tilde{m}^2} &= \chi_{\tilde{m}^2 \tilde{m}^{\dagger,2}} \\ &= \frac{[1 + (g_0 - 2v_{\mathbf{q}})A_0](g_2 b_2^2 - g_2 d_2^2 - d_2) + 2(g_0 - 2v_{\mathbf{q}}) c_1^2 [2 g_2 (b_2 - d_2) - 1]}{D_0 D_2'}. \end{aligned} \tag{30}$$

The density response function $\chi_{\rho\rho}$ given by (23) is of special interest. Using the expressions (B3) in Appendix B which are valid for $\mathbf{q} = 0$, one can easily verify that the numerator of $\chi_{\rho\rho}$ vanishes and hence

$$\chi_{\rho\rho}(\mathbf{q} = 0, \omega) = 0. \tag{31}$$

Thus the density response function we obtain satisfies the requirement of particle number conservation.[11] All other response functions in (15) which are not listed above vanish in the small-$\mathbf{q}$ limit, even in the absence of the Coulomb interaction.

We observe that the d-wave pair-pair response functions in (29) and (30) clearly have the same collective mode spectrum as the density response function in (23). The phase fluctuations of the d-wave order parameter couple into the density fluctuation spectrum and are given by the zeros of D_0 in (20), which are strongly modified by the Coulomb interaction.

III. COLLECTIVE MODE SPECTRUM AND DAMPING

A. BCS particle-hole continuum

As mentioned in Sec. I, the d-wave order parameter is anisotropic with nodes at the Fermi surface and therefore the quasiparticle energies and the two-particle spectrum are strongly dependent on the direction of the momentum $\mathbf{q}$. The BCS "particle-hole" continuum (at T=0) is given by $\omega_{p\text{-}h} = E_{\mathbf{p}} + E_{\mathbf{p}+\mathbf{q}}$ corresponding to the minimum energy required to break a Cooper pair. If we assume that the dominant contribution in the calculation of various correlation function comes from quasiparticles with momentum near the Fermi wave vector ($|\mathbf{p}| = k_F$), we find

$$\begin{aligned} \omega_{p\text{-}h} = |\Delta \cos(2\phi')| + [v_F^2 q^2 \cos^2(\phi - \phi') \\ + \Delta^2 \cos^2(2\phi')]^{\frac{1}{2}}. \end{aligned} \tag{32}$$

Here ϕ' is defined as the angle between the quasiparticle momentum $\mathbf{p}$ and $\mathbf{k}_x$ axis, ϕ is defined as the angle between $\mathbf{q}$ and $\mathbf{k}_x$ axis (see Fig. 1), and the long-wavelength limit ($|\mathbf{q}| \ll k_F$) has been assumed,

$$\epsilon_{\mathbf{p}+\mathbf{q}} \simeq \mathbf{v}_F \cdot \mathbf{q} \ , \qquad \Delta_{\mathbf{p}+\mathbf{q}} \simeq \Delta_{\mathbf{p}} = \Delta \cos(2\phi'). \tag{33}$$

We examine two extreme cases. When $\mathbf{q}$ is along the direction of $\phi = 0$, where the magnitude of the order parameter is maximum, one finds that there is a lower and upper limit for $\omega_{p\text{-}h}$ in (32), i.e.,

$$\omega_{1,\phi=0}(q) \le \omega_{p\text{-}h,\phi=0}(\mathbf{q}) \le \omega_{2,\phi=0}(q). \tag{34}$$

Here we have defined the boundary frequencies by

$$\omega_{1,\phi=0}(q) \equiv \frac{v_F q}{\sqrt{2}} \tag{35}$$

and

$$\omega_{2,\phi=0}(q) \equiv \Delta(1 + \sqrt{1 + v_F^2 q^2/\Delta^2}\ ). \tag{36}$$

Clearly $\omega_{1,\phi=0}(q)$ is the minimum energy required to break a Cooper pair and the particle-hole excitation band is thus bounded by $\omega = \omega_{1,\phi=0}(q)$ and $\omega = \omega_{2,\phi=0}(q)$ for given momentum $\mathbf{q}$ with $\phi = 0$ (see Fig. 2). In general, for the spectrum of p-h modes in 2D d-wave superconductors, two different regions are obtained, separated by the dispersion relation $\omega = \omega_{1,\phi=0}(q)$. For $\omega > \omega_{1,\phi=0}(q)$, the p-h spectral weight is finite and collective modes found in this region are damped. In contrast, for $\omega < \omega_{1,\phi=0}(q)$, the p-h spectral weight is zero and collective modes appearing in this region will be undamped.

For $\mathbf{q}$ along the direction $\phi = \pi/4$, where the order parameter vanishes (nodes), one finds, using approximation (33),

$$0 \le \omega_{p\text{-}h,\phi=\pi/4}(q) \le \omega_{2,\phi=\pi/4}(q), \tag{37}$$

where

$$\omega_{2,\phi=\pi/4}(q) \equiv \Delta(1 + \sqrt{1 + v_F^2 q^2/2\Delta^2}\ ). \tag{38}$$

The minimum value of $\omega_{p\text{-}h,\phi=\pi/4}(q)$ is zero, a direct result of there being no pair breaking gap. The p-h spectral weight is therefore finite at any frequency and collective modes are always damped. However, the p-h spectral weight in the region $\omega \le \omega_{1,\phi=\pi/4}(q) \equiv v_F q$ is much smaller (as long as $v_F q \ll 2\Delta$) than in the region of

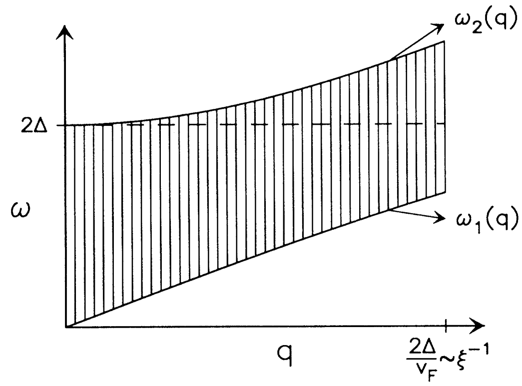

FIG. 2. Schematic rendering of the particle-hole continuum in a 2D BCS d-wave superconductor (hatched area). These are for the direction of $\mathbf{q}$ with $\phi = 0$, where the magnitude of the order parameter is maximum (see Fig. 1). The lower edge of the p-h band at $\omega_1^2 = \frac{1}{2}v_F^2 q^2$ corresponds to the minimum energy required to break up a Cooper pair of momentum $\mathbf{q}$.

$\omega > \omega_{1,\phi=\pi/4}(q)$. This implies that long-wavelength collective modes for $\phi = \pi/4$ with low energy may be weakly damped and hence observable.

It is of interest to evaluate the imaginary part of the density response function for two noninteracting BCS quasiparticles [see (23) for $g_0 = g_2 = v_{\mathbf{q}} = 0$],

$$\mathrm{Im}\chi^0_{\rho\rho} \sim \mathrm{Im}[\overline{f_0 f_0 \widetilde{G}_{11}\widetilde{G}_{11}} - \overline{f_0 f_0 \widetilde{G}_{12}\widetilde{G}_{12}}] = \mathrm{Im}A_0. \quad (39)$$

Results are shown for this in Fig. 3 at finite $\mathbf{q}$ for both $\phi = 0$ and $\pi/4$. The spectral density in (39) should be of direct physical interest in phonon self-energies and other experimental quantities. Due to the anisotropy of the d-wave order parameter, the noninteracting two-particle spectrum described by (39) is strongly dependent on the direction of $\mathbf{q}$, particularly at the region of $\omega \sim 2\Delta$. One finds that two cusps in the $\phi = 0$ case collapse into a single cusp in the $\phi = \pi/4$ case. The two cusps for $\phi = 0$ correspond to $\omega = 2\Delta$ and $\omega = \omega_{2,\phi=0}$ as defined in (36). The single cusp for $\phi = \pi/4$ corresponds to $\omega = \omega_{2,\phi=\pi/4}$ in (38). This anisotropic p-h spectrum at finite $\mathbf{q}$ is a characteristic feature of 2D d-wave superconductors. We also note that while the p-h spectral weight develops from $\omega = 0$ for the $\phi = \pi/4$ case, the weight is much smaller for $\omega \leq \omega_{1,\phi=\pi/4}(q)$ compared to the weight for $\omega > \omega_{1,\phi=\pi/4}(q)$.

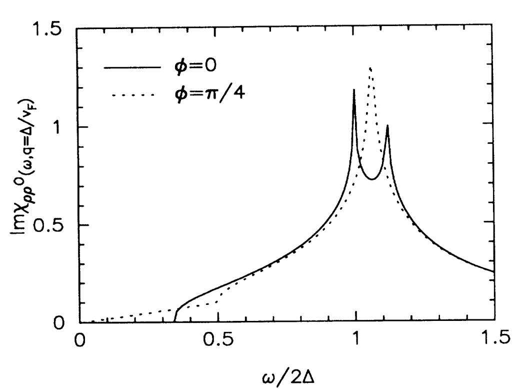

FIG. 3. The frequency dependence of the imaginary part of the noninteracting density response function $\mathrm{Im}\chi^0_{\rho\rho}(\mathbf{q},\omega) \propto \mathrm{Im}A_0$, as defined in (23) and (39), for $q = \Delta/v_F$ and two different directions of $\mathbf{q}$.

B. Collective fluctuation spectrum in the L=0 channel ($D_0 = 0$)

Using the long-wavelength approximation results derived in Appendix B, we find that the phase fluctuation modes are given by the zeros of the real part of [we redefine $N(0)g_0 \to g_0$ and $N(0)g_2 \to g_2$]

$$\begin{aligned} D_0(q,\omega) = &\left[1 - 2g_0 I_2(\bar\omega) + g_0 A_0''(\bar\omega)\frac{s^2q^2}{\Delta^2}\right] \\ &\times \left[4\bar\omega^2 g_2 I_2(\bar\omega) + g_2 B_2''(\bar\omega)\frac{s^2q^2}{\Delta^2}\right] \\ &+8g_0g_2\bar\omega^2\left[I_2(\bar\omega) + c_1''(\bar\omega)\frac{s^2q^2}{\Delta^2}\right]^2, \end{aligned} \quad (40)$$

where we define $A_L''(\omega) \equiv a_L''(\omega) - b_L''(\omega)$ and $B_L''(\omega) \equiv b_L''(\omega) + d_L''(\omega)$ (see Appendix B) and $s \equiv v_F/\sqrt{2}$. Here we ignore the bubble diagrams due to the Coulomb interaction ($v_{\mathbf{q}} = 0$). Since we are interested in the low-frequency region $\omega \ll 2\Delta$, terms of order $\omega^2(s^2q^2)/\Delta^4$, s^4q^4/Δ^4 and higher-order terms can be neglected and thus (40) reduces to

$$D_0(q,\omega) = 4\bar\omega^2 g_2 I_2(\bar\omega) + [1 - 2g_0 I_2(\bar\omega)]g_2 \bar B_2''(\bar\omega)\frac{s^2q^2}{\Delta^2}, \quad (41)$$

where the function $\bar B_2''$ is (see Appendix B)

$$\bar B_2''(\bar\omega) = \frac{1}{2}J_{431}(\bar\omega) + J_{211}(\bar\omega) + 8J_{2-12}(\bar\omega) - 4J_{412}(\bar\omega). \quad (42)$$

To go further in this analysis, numerical studies are needed. It turns out that when $\omega \ll 2\Delta$, the imaginary component of $D_0(q,\omega)$ in (41) is negligibly small and $\mathrm{Re}I_2(\bar\omega) \simeq -\mathrm{Re}\bar B_2''(\bar\omega) \simeq 1/4$. We therefore obtain a well defined phononlike dispersion relation

$$\begin{aligned} \omega^2 &\simeq [1 + 2\mathrm{Re}\bar B_2''(\bar\omega)g_0]s^2q^2 \\ &\simeq \left(1 - \frac{1}{2}g_0\right)s^2q^2, \end{aligned} \quad (43)$$

a result only valid for $q \lesssim \Delta/v_F$. This describes the phase fluctuations of the d-wave order parameter which are coupled into the density fluctuations (since it occurs in the L=0 channel). This phononlike mode is the analog of the well-known Anderson–Bogoliubov (AB) mode in s-wave superconductors.[9,17,18] One notes that g_0 has no effect on the acoustic dispersion relation of this mode, apart from renormalizing the sound velocity.

The effect of the Coulomb interaction can be easily included by replacing g_0 in (43) by $g_0 - 2v_\mathbf{q}$ [here $v_\mathbf{q}$ is really $N(0)v_\mathbf{q}$]. One finds that the phonon mode in (43) is then renormalized to

$$\omega^2 = \omega_{2\text{D}}^2 + \left(1 - \frac{1}{2}g_0\right) s^2 q^2, \tag{44}$$

where $\omega_{2\text{D}}^2 \equiv 2\pi n e^2 q/m$ ($n = k_F^2/2\pi$ is the 2D number density) dominates in the rhs of (44) at low $\mathbf{q}$. This is recognized as the dispersion relation of a 2D plasmon. This behavior is, of course, expected for all BCS superconductors, independent of the pairing symmetry.[17,18] We note that, as recently discussed in detail by CG (Ref. 9) in the case of s-wave superconductors, while plasmons can exist above 2Δ as well as below 2Δ in 2D superconductors, their physical origin is quite different in the two regions.

Although the phonon is renormalized into a 2D plasmon due to the long-range Coulomb interaction, it is interesting to study how the phononlike mode which appears in a "neutral" superconductor depends on $\mathbf{q}$. In the lower L=0 spectrum in Fig. 4, the two extreme cases ($\phi = 0$ and $\pi/4$) for the direction of $\mathbf{q}$ are shown. We take $g_2 = -0.25$, and set $g_0 = g_2$ as g_0 only modifies the phonon velocity. One can see that up to $q \sim \Delta/v_F$, the phonon frequency is not very sensitive to the direction of the propagation wave vector $\mathbf{q}$.

C. Collective fluctuation spectrum in the L=2 channel ($D_2 = 0$)

The L=2 channel is of most interest in Raman scattering (see Sec. IV). We consider $\mathbf{q} = 0$ at T=0. The collective modes in this channel are given by the solution of $\text{Re}D_2(\omega) = 0$, where D_2 is defined in (21). Using the results in Appendix B again, D_2 can be reduced to [as usual, with $N(0)g_0 \to g_0$, and $N(0)g_2 \to g_2$]

$$D_2(\omega) = [1 - 2g_2 I_4(\bar\omega)]\left[1 - \frac{g_0}{g_2} + 4g_0\bar\omega^2 I_0(\bar\omega)\right] + 8g_0 g_2 \bar\omega^2 I_2^2(\bar\omega). \tag{45}$$

In general, the functions $I_i(\omega)$ defined in (B4) have imaginary components in all frequency regions since pair breaking can occur at energies below as well as above 2Δ. We may rewrite (45) in the form

$$D_2(\omega) = [1 - 2g_2 I_4(\bar\omega)][1 - g_0 R(g_2, \bar\omega)], \tag{46}$$

where R is defined by

$$R(g_2, \bar\omega) = \frac{1}{1 - 2g_2 I_4(\bar\omega)}\left[[1 - 2g_2 I_4(\bar\omega)] \times \left(\frac{1}{g_2} - 4\bar\omega^2 I_0(\bar\omega)\right) - 8g_2\bar\omega^2 I_2^2(\bar\omega)\right]. \tag{47}$$

Using (46), collective modes in this channel are given by the solutions of

$$\frac{1}{g_0} = \text{Re}R(g_2, \bar\omega). \tag{48}$$

Noting the definition of R in (47), we see that there is no zero of D_2 in (46) due to the vanishing of the factor $[1 - 2g_2 I_4(\bar\omega)]$.

The solutions of (48) will be referred to as "excitonlike" modes, the analog of those found by Bardasis and Schrieffer[12] in 3D s-wave superconductors (see Appendix C). The solutions with $g_0 < 0$ correspond to "particle-particle"-type excitonlike modes, while the solutions with $g_0 > 0$ correspond to "particle-hole"-type excitonlike modes. In physical terms, when a d-wave Cooper pair (formed by the dominant g_2 pairing) breaks up into two quasiparticles, the so-called "residual attractive interaction" g_0 leads to the formation of a new (excited-state) bound pair, somewhat analogous to the electron-hole pairs (excitons) in semiconductors. These high-energy excited-state bound pairs behave like particles with finite center-of-mass momentum and do not form part of the "Bose condensate" associated with the ground-state Cooper pairs.

For given (real) values of ω and g_2, we can solve for the value of g_0 which satisfies (48). The results are presented in the top line of Fig. 5 for T=0. We obtain particle-particle-type excitons in d-wave superconductors with an energy below 2Δ when $\mathbf{q} = 0$ (i.e., when the excited bound state has no center-of-mass kinetic energy). At T=0, these excitons have an energy gap (i.e., are massive). In Fig. 5, this gap is at $\omega_g = 0.9(2\Delta)$ for $|g_0| = |g_2| \equiv 0.25$. Within this gap [$\omega \leq 0.9(2\Delta)$], the only solution of (48) for real ω requires that $|g_0| > |g_2|$, which is not possible in a d-wave superconductor.

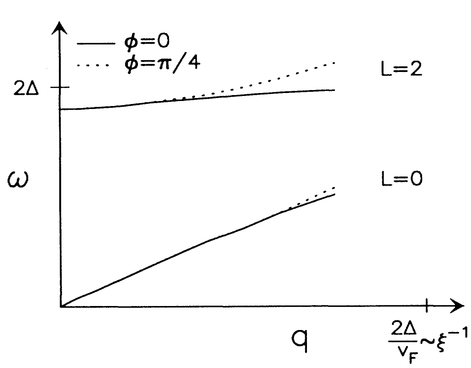

FIG. 4. The dispersion relation of the collective modes in a 2D d-wave "neutral" superconductor for both L=0 and 2 channels. Two different angles for the wave vector $\mathbf{q}$ are shown. For both channels (L=0,2), we set $g_0 = g_2 = -0.25$. The frequencies associated the excitonlike mode (upper curve) for the two propagation directions start to significantly deviate from each other for $q \sim \Delta/v_F$.

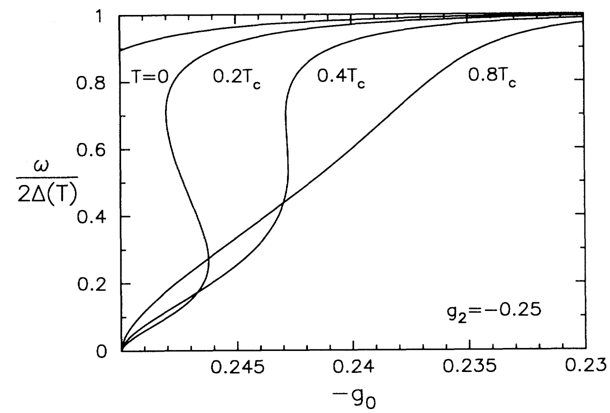

FIG. 5. The frequency of the $\mathbf{q} = 0$ excitonlike modes in a 2D d-wave superconductor vs the magnitude of attractive g_0 (< 0), at various temperatures. These results are for $g_2 = -0.25$.

As the d-wave order parameter is anisotropic with nodes on the Fermi surface, BCS particle-hole excitations can exist at any frequency below 2Δ at specific directions and points on the Fermi surface (in the s-wave case,[9] in contrast, the BCS p-h excitation spectrum only appears for $\omega \geq 2\Delta$). This means that all the functions $I_i(\bar{\omega})$ appearing in (45) have imaginary components, which in turn means that these excitonlike collective modes are always damped (to a lesser or greater degree).

The solutions of (48) in the case of finite temperature have also been investigated (see Fig. 5). Since the $\mathbf{q} = 0$ case is considered, the only change needed in the calculation at finite temperatures is to replace the $I_i(\bar{\omega})$ in (45) by

$$I_i(\bar{\omega}) \to I_i(\bar{\omega},T) \equiv -\frac{1}{16}\int_{-\infty}^{\infty} d\bar{\epsilon} \int_0^{2\pi} \frac{d\phi'}{2\pi} \frac{|f_2(\hat{\mathbf{p}})|^i}{\bar{E}(\bar{\omega}^2 - \bar{E}^2)} \times \tanh\left(\frac{\beta E_{\mathbf{p}}}{2}\right), \tag{49}$$

where $\beta = 1/k_BT$, $\bar{\epsilon} \equiv \epsilon/\Delta(T)$, $\bar{E} \equiv E/\Delta(T)$, and $\bar{\omega} \equiv \omega/2\Delta(T)$. Note that in Fig. 5, the frequency ω is scaled to the temperature-dependent order parameter; i.e., the energy range for each curve (each temperature) is different. For a given value of the attractive pairing interaction g_0, with a fixed value of g_2 the energy of the collective mode solution of (48) is found to *decrease* as the temperature increases. This decrease is largest when the system has a strong residual interaction g_0 (although not sufficiently large to break the d-wave superconductivity). One finds that the damping in the low-frequency region is much smaller than in the high-frequency region $\sim 2\Delta$, which implies that these excitonlike modes are well defined at higher temperatures. This is of interest in Raman-scattering experiments (see Sec. IV). More generally, the results in Fig. 5 show that the energy gap at T=0 is removed at finite temperatures.

We have also numerically evaluated the excitonlike mode frequency for $q \sim \Delta/v_F$ and T=0 (see the upper L=2 spectrum in Fig. 4). Again, the two extreme cases of $\phi = 0$ and $\pi/4$ for the direction of $\mathbf{q}$ are considered. Here we choose $g_0 = g_2 = -0.25$, as representative values. For the two different values of ϕ, the two different frequencies only start to differ significantly when $q \gtrsim \Delta/v_F$.

D. Collective fluctuation spectrum in $D'_\ell = 0$ (ℓ=0,2)

In a s-wave superconductor ($\Delta_{\mathbf{p}} = \Delta$), it is $\tilde{m}^{L=0} \equiv m$ which corresponds to the BCS order parameter.[9] The pair-pair correlation functions are described by the analog of $\chi_{\tilde{m}^{\dagger,0}\tilde{m}^{\dagger,0}}$ in (27) or $\chi_{\tilde{m}^{\dagger,0}\tilde{m}^0}$ in (28) and have a denominator involving D'_0 [defined in (22)] which is clearly unaffected by the Coulomb interaction. One may easily check that the zeros of D'_0 correspond to the amplitude modes discussed by Littlewood and Varma.[19] In particular, $D'_0(\mathbf{q} = 0, \omega = 2\Delta) = 0$ reduces to the s-wave gap equation. At low $\mathbf{q}$, the amplitude mode is found to have the dispersion relation (in 2D)

$$\omega^2 = (2\Delta)^2 + \frac{1}{2}(v_F q)^2. \tag{50}$$

While $\chi_{\tilde{m}^{\dagger,2}\tilde{m}^{\dagger,2}}$ in (29) and $\chi_{\tilde{m}^{\dagger,2}\tilde{m}^2}$ in (30) have denominators involving D'_2, there is no solution for real ω of $D'_2 = 0$ for s-wave superconductors (we note that $D'_2 = 1$ if $g_2 = 0$).

In contrast, in a d-wave superconductor, it is $\tilde{m}^{L=2}$ which corresponds to the BCS order parameter involved in the gap equation. Consequently it is $\chi_{\tilde{m}^{\dagger,2}\tilde{m}^{\dagger,2}}$ or $\chi_{\tilde{m}^{\dagger,2}\tilde{m}^2}$ which describes the order parameter fluctuations. As a result, we would expect that the amplitude fluctuations of the order parameter will be given by the zeros of D'_2 in (22), the explicit form being given by

$$D'_2 = 1 + g_2 \int \frac{d\mathbf{p}}{(2\pi)^2} |f_2(\hat{\mathbf{p}})|^2 \frac{E + E'}{2EE'} \times \frac{\Delta_{\mathbf{p}}\Delta_{\mathbf{p}+\mathbf{q}} - EE' - \epsilon\epsilon'}{\omega^2 - (E+E')^2}. \tag{51}$$

Thus for $\mathbf{q} = 0$, the zeros of D'_2 are given by the solutions of

$$1 + g_2 \int \frac{d\mathbf{p}}{(2\pi)^2} |f_2(\hat{\mathbf{p}})|^2 \frac{1}{2E} \frac{-4(E^2 - |\Delta_{\mathbf{p}}|^2)}{\omega^2 - 4E^2} = 0. \tag{52}$$

Using the d-wave gap equation (B6), one finds that (52) has a solution $\omega^2 = \langle |f_2(\hat{\mathbf{p}})|^2 (2\Delta_{\mathbf{p}})^2 \rangle = 3\Delta^2$, where the angular average $\langle\ \rangle$ is over the Fermi surface. This amplitude mode is clearly the d-wave generalization of the s-wave amplitude mode[19] given by (50), involving an appropriate Fermi surface average of the minimum energy $2\Delta_{\mathbf{p}}$ of two quasiparticles. This amplitude mode is, as expected, strongly damped due to the p-h breaking. While the correlation functions (27) and (28) involving $\tilde{m}^{L=0} = m$ and $m^\dagger$ have D'_0 in the denominator, we find no solutions of Re$D'_0 = 0$ for real ω in a d-wave superconductor (also note that $D'_0 = 1$ for $g_0 = 0$).

IV. RAMAN-SCATTERING INTENSITY ($\mathbf{q} \to 0$)

A. Raman response functions

In order to illustrate how the collective fluctuations in 2D superconductors affect physical quantities, we now consider the Raman-scattering intensity in connection with the formalism derived in Sec. II. As discussed at length in the literature,[20,21,23,24] Raman scattering involves a light-scattering experiment in the $\mathbf{q} = 0$ limit which can probe different symmetries by choosing appropriate incident and scattered polarization directions of photons. As discussed in these references, it is convenient to introduce an "effective density" operator

$$\tilde{\rho}_{\mathbf{q}} \equiv \sum_{\mathbf{p},\sigma} \gamma_{\mathbf{p}}(\mathbf{q}) a^{\dagger}_{\mathbf{p},\sigma} a_{\mathbf{p}+\mathbf{q},\sigma}, \tag{53}$$

where $\gamma_{\mathbf{p}}$ is the Raman-scattering strength. The cross section for Raman scattering is then given by[23]

$$\widetilde{S}(\mathbf{q},\omega) = -\frac{1}{\pi}[1+n_B(\omega)]\mathrm{Im}\chi_{\tilde{\rho}\tilde{\rho}}(\mathbf{q}, i\omega_n \to \omega + i\delta), \tag{54}$$

where $n_B(\omega) = [\exp(\beta\omega) - 1]^{-1}$ is the Bose distribution function and the Raman response function is defined in terms of the effective density operators in the usual way,

$$\chi_{\tilde{\rho}\tilde{\rho}}(\mathbf{q}, i\omega_n) = -\int_0^{\beta} d\tau e^{i\omega_n\tau} \langle \hat{\mathrm{T}}_{\tau} \tilde{\rho}_{\mathbf{q}}(\tau) \tilde{\rho}^{\dagger}_{\mathbf{q}}(0)\rangle. \tag{55}$$

The $\mathbf{q}$ dependence of the Raman-scattering strength $\gamma_{\mathbf{p}}$ is dropped since we are in the $\mathbf{q} \to 0$ limit. One can therefore expand $\gamma_{\mathbf{p}}$ in (53) in terms of orthogonal angle functions $f_L(\hat{\mathbf{p}})$,[20,23]

$$\gamma_{\mathbf{p}} = \sum_L \gamma_L f_L(\hat{\mathbf{p}}), \tag{56}$$

which is dependent on the direction of $\mathbf{p}$ only. By using (56), one can rewrite the effective density $\tilde{\rho}_{\mathbf{q}}$ in (53) as

$$\tilde{\rho}_{\mathbf{q}} \equiv \sum_L \gamma_L \tilde{\rho}^L_{\mathbf{q}}, \tag{57}$$

where the L-dependent $\tilde{\rho}^L_{\mathbf{q}}$ are defined earlier in (7). As a result, the Raman-scattering cross section can be decoupled into various channels in the limit of $\mathbf{q} \to 0$, i.e.,

$$\widetilde{S}(\mathbf{q}\to 0,\omega) \equiv -\frac{1}{\pi}[1+n_B(\omega)]\sum_L |\gamma_L|^2 \widetilde{S}^L(\mathbf{q}\to 0,\omega), \tag{58}$$

where the off-diagonal terms ($L \neq L'$) make a negligible contribution to (58) (at $\mathbf{q} \to 0$). Here $|\gamma_L|^2$ gives the diagonal ($L = L'$) scattering strength in the L channel. The L-channel Raman-scattering cross section is proportional to the imaginary component of the L-channel effective density-density correlation function, namely,

$$\widetilde{S}^L(\mathbf{q}\to 0,\omega) \equiv \widetilde{S}^L(\omega) = \mathrm{Im}\chi_{\tilde{\rho}^L\tilde{\rho}^L}(\mathbf{q}\to 0,\omega). \tag{59}$$

We recall from Sec. II that the full correlation functions which determine the Raman-scattering intensities in (58) and (59) are given by

$$\chi_{\tilde{\rho}^0\tilde{\rho}^0} = \frac{A_0(1+g_2B_2)+4g_2c_1^2}{D_0} \tag{60}$$

in (23) and

$$\chi_{\tilde{\rho}^2\tilde{\rho}^2} = \frac{A_2(1+g_0B_0)+4g_0c_1^2}{D_2} \tag{61}$$

in (24),where D_0 and D_2 are defined in (20) and (21). It was shown there that only $\chi_{\tilde{\rho}^0\tilde{\rho}^0}$ is modified by the Coulomb interaction, while $\chi_{\tilde{\rho}^2\tilde{\rho}^2}$ is not. The result in (60) shows that poles may occur when $D_0 = 0$, which correspond to collective modes in the L=0 channel discussed earlier in Sec. III. Similarly, the result in (61) gives poles at $D_2 = 0$, which correspond to the collective modes in the L=2 channel.

As with s-wave superconductors,[9,24] it is convenient to rewrite (60) and (61) in the form

$$\chi_{\tilde{\rho}^L\tilde{\rho}^L} \equiv \chi^L_{\tilde{\rho}\tilde{\rho}}(\mathbf{q},\omega) = \frac{R_L}{1+V_LR_L}, \tag{62}$$

where $V_L \equiv g_L - 2v_{\mathbf{q}}\delta_{0,L}$ and the functions R_L (L=0,2) are now defined by

$$R_L \equiv A_L + \frac{g_{L'}(2c_1)^2}{1+g_{L'}B_{L'}}. \tag{63}$$

Here L'=2 when L=0, and *vice versa.* (In s-wave superconductors, one has $L' = L$.) By writing (62) in this form, the physics involved in the Raman-scattering cross section will be more transparent. More generally, using (59) in conjunction with (62), we have

$$\widetilde{S}^L(\omega) \equiv -\frac{1}{V_L}\mathrm{Im}\left[\frac{1}{1+V_LR_L(\omega)}\right] = \frac{\mathrm{Im}R_L(\omega)}{[1+V_L\mathrm{Re}R_L(\omega)]^2+[V_L\mathrm{Im}R_L(\omega)]^2}. \tag{64}$$

In d-wave superconductors, since the order parameter is anisotropic with nodes at the Fermi surface, $\mathrm{Im}R_L(\omega)$ can be large at frequencies below 2Δ. Any peak associated with the collective modes as defined here will be strongly damped by the large imaginary component of R_L. However, we shall see later that $\widetilde{S}^L(\omega)$ in (64) can still exhibit a broad resonance or structure arising from the frequency dependence of $R_L(\omega)$ in (64). Moreover, at high temperatures ($T \gtrsim 0.7T_c$), collective modes in the L=2 channel are weakly damped if g_0 is comparable to g_2, and as a result, can give rise a peak in the L=2 Raman-scattering intensity. In contrast, these modes are completely washed out at low temperatures ($T \ll T_c$), where most Raman experiments have been carried out.

Considering the cuprate oxides with the symmetry of the D_{4h} point group, to a good approximation, one has the following symmetry channels for the Raman-scattering strength in (56):[11]

$$\gamma_{\mathbf{p}}^{s} = \begin{cases} \gamma_s^0 + \gamma_s^1 \cos(4\phi), & s = A_{1g}, \\ \gamma_s \cos(2\phi), & s = B_{1g}, \\ \gamma_s \sin(2\phi), & s = B_{2g}, \end{cases} \tag{65}$$

where s denotes the symmetry which is studied in a particular Raman-scattering geometry. Here γ_s^0 represents the isotropic and γ_s^1 represents the anisotropic component of γ_s, while ϕ is the direction of $\mathbf{p}$ on the 2D circular Fermi surface.

B. Raman intensity

In the $\mathbf{q} \to 0$ limit, the L=0 channel has $V_0 \equiv g_0 - 2v_{\mathbf{q}} \to -\infty$. In view of the factor $1/V_L$ in $\widetilde{S}^L(\omega)$ in (64), the Raman intensity in the (isotropic) L=0 channel is completely screened by the Coulomb interaction. In other words, there is no weight for the 2D plasmon mode, although it has low frequency ($\propto \sqrt{q}$) which makes it potentially more interesting than 3D plasmons. As a result, the Raman intensity of A_{1g} symmetry will be partially screened by the Coulomb interaction due to the existence of the L=0 isotropic component in $\gamma_{A_{1g}}$ [see (65)].

In contrast, since $V_2 = g_2$, the L=2 channel Raman intensity is not screened at all by the Coulomb interaction. Since the L=2 channel corresponds to $f_2(\hat{\mathbf{p}}) \sim \cos(2\phi)$, the following Raman intensities for the L=2 channel are all of B_{1g} symmetry [see (65)]. Substituting (B3) into (63), one obtains for the L=2 channel (at T=0)

$$R_2(\omega) = -2I_4(\bar{\omega}) + \frac{8g_0\bar{\omega}^2 I_2^2(\bar{\omega})}{1 + g_0[-1/g_2 + 4\bar{\omega}^2 I_0(\bar{\omega})]}. \tag{66}$$

We recall from (64) that the complete L=2 Raman scattering intensity is given by

$$\widetilde{S}^{L=2}(\bar{\omega}) = \mathrm{Im}\left[\frac{R_2(\omega)}{1 + g_2 R_2(\omega)}\right], \tag{67}$$

and thus the function $\mathrm{Im}R_2(\omega)$ is directly proportional to the spectral weight for L=2 Raman-scattering intensity. When we set $g_0 = g_2 = 0$, (66) and (67) give

$$\widetilde{S}^{L=2}(\bar{\omega}) = \mathrm{Im}R_2(\omega) = -2\mathrm{Im}I_4(\bar{\omega}). \tag{68}$$

This result gives a single peak at $\omega = 2\Delta$ and goes as $\sim \omega^3$ in the low-frequency region (see Fig. 6). This choice corresponds to the neglect of ladder diagrams (vertex corrections), which are the source of the condensate collective fluctuations we are considering.

Keeping only g_2 (but $g_0 = 0$), we obtain

$$\widetilde{S}^{L=2}(\bar{\omega}) = \mathrm{Im}\left[\frac{-2I_4(\bar{\omega})}{1 - 2g_2 I_4(\bar{\omega})}\right] \simeq -2\mathrm{Im}I_4(\bar{\omega}), \tag{69}$$

where the last step makes use of the fact that $|2g_2 I_4(\bar{\omega})| \ll 1$ in most of the frequency region of interest (except for ω near 2Δ). Comparing (68) and (69), one sees that there is little difference in the Raman intensity (see Figs. 6 and 7) from the case when vertex corrections are completely neglected. Thus we see that a finite value

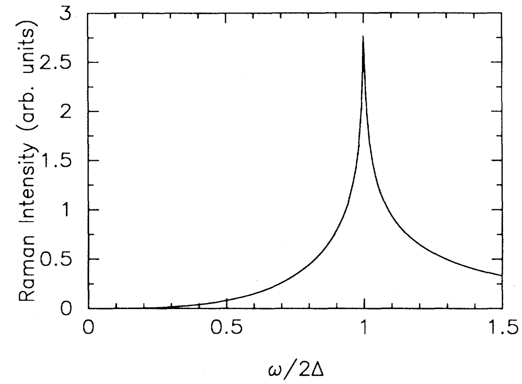

FIG. 6. The intensity of the $\mathbf{q} = 0$ L=2 channel Raman-scattering (at T=0) in a 2D d-wave superconductor as a function of frequency, ignoring all vertex corrections ($g_0 = g_2 = 0$).

of g_0 plays a key role in the L=2 Raman-scattering intensity. For small values of g_0, one finds that there is no drastic change in the Raman intensity (see Fig. 7) from the $g_0 = 0$ case, apart from a decrease in the intensity of peak around 2Δ (where the pair breaking mechanism is strongest). However, when g_0 is large (but $|g_0| < |g_2|$), the low-frequency intensity goes as $\sim \omega$, rather than as $\sim \omega^3$. Observation of such a change would give direct evidence that there is a strong s-wave pairing interaction in d-wave superconductors.

We note that at T=0, the excitonlike modes discussed earlier in Sec. III are completely washed out due to the large imaginary part of correlation functions in this frequency region. [We recall from Fig. 5 (T=0 case), for example, for $g_0 = -0.249$ and $g_2 = -0.250$, that we found a collective mode at $\omega \simeq 0.92(2\Delta)$ at $\mathbf{q} = 0$.] The large damping in the Raman spectrum is a direct consequence of the fact there is no forbidden frequency region in an anisotropic d-wave superconductor at $\mathbf{q} = 0$ (no pair breaking gap). However, the T=0 Raman spectrum still exhibits some important characteristic features (see

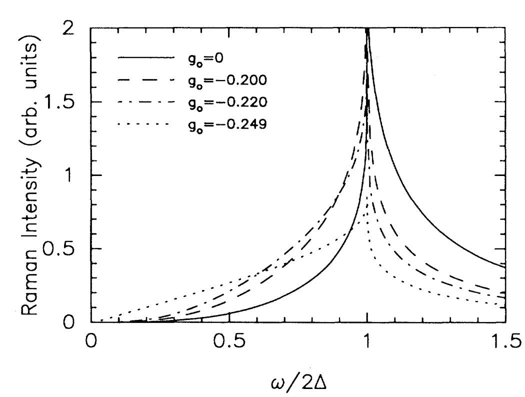

FIG. 7. The intensity of the $\mathbf{q} = 0$ L=2 channel Raman-scattering (at T=0) for a 2D d-wave superconductor as a function of frequency, for several values of g_0 (< 0) and a fixed value of $g_2 = -0.25$.

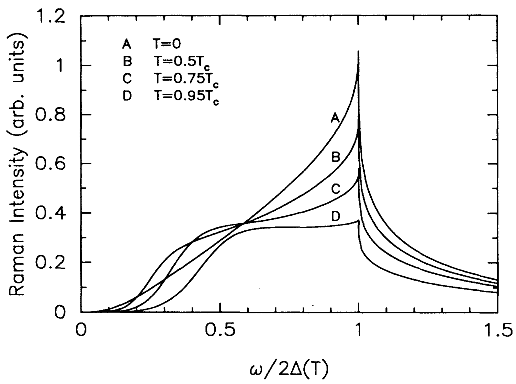

FIG. 8. The intensity of the $\mathbf{q} = 0$ L=2 channel Raman-scattering for a 2D d-wave superconductor at various temperatures, for $g_0 = -0.24$, setting $g_2 = -0.25$.

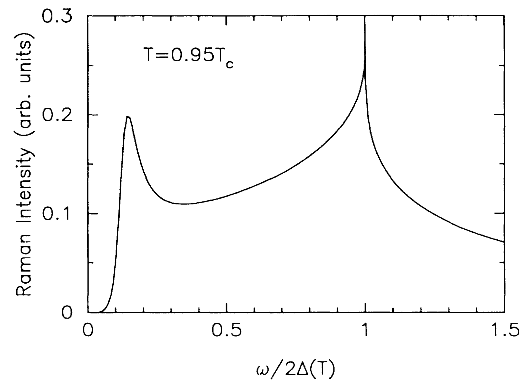

FIG. 10. The L=2 channel Raman-scattering intensity at $T = 0.95T_c$ (taken from Fig. 9).

Fig. 7) in the low-frequency region which result from the vertex corrections.

Some finite-temperature results are shown in Figs. 8–10. It is clear that the Raman spectrum becomes very temperature dependent when g_0 is appreciable. Unless g_0 is comparable to g_2, the intensities do not change much with temperature, except that the intensity of the peak at 2Δ decreases strongly near T_c (see Fig. 8). In particular, when $T = 0.95T_c$, the peak at $2\Delta(T)$ almost disappears, leading to a flat spectrum at $\omega \lesssim 2\Delta(T)$. However, one sees some structure developing at low-frequencies. When the magnitude of the residual interaction g_0 is close in magnitude to g_2 (see Figs. 9 and 10), a strong peak [comparable in intensity to the pair-breaking peak at $2\Delta(T)$] can arise at low frequencies ($\omega \ll 2\Delta$) as the temperature increases. In fact, this peak corresponds precisely to the excitonlike collective mode whose frequency is shown at finite temperatures in Fig. 5. The damping is much smaller in the low-frequency region [$\omega \ll 2\Delta(T)$] compared to the high-frequency region [$\omega \lesssim 2\Delta(T)$] and therefore these excitonlike modes develop weight in the Raman-scattering intensity when their frequency is shifted downward. We find that the strongest low-frequency peak occurs at $T \simeq 0.75T_c$, at a frequency $\omega \simeq 0.2\Delta(T)$ (see Fig. 9). This feature in d-wave superconductors may be useful in distinguishing high-T_c materials in which there is a significant s-wave pairing interaction (phonon induced, for example).

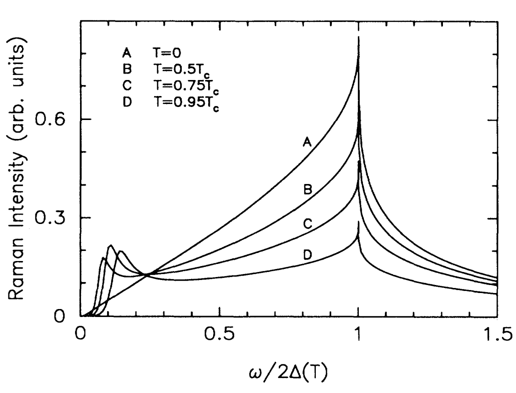

FIG. 9. The intensity of the $\mathbf{q} = 0$ L=2 channel Raman-scattering for a 2D d-wave superconductor at various temperatures, for $g_0 = -0.249$ and $g_2 = -0.250$.

V. CONCLUSIONS

We have studied the collective modes and Raman-scattering intensity for a 2D spin-singlet d-wave superconductor, assuming both s- and $d_{x^2-y^2}$-wave contributions to the pairing interaction. We have shown that the Cooper pair condensate fluctuations in d-wave superconductors can lead to several characteristic features which can be experimentally distinguished from those in s-wave superconductors.

In d-wave superconductors, the long-range Coulomb interaction turns the phonon modes in the L=0 channel into plasmon modes, as one expects from very general considerations in all BCS-type superconductors. We show explicitly that the Coulomb interaction has no effect on the other modes. The excitonlike modes (which occur in the L=2 channel) are strongly damped at T=0. However, we have shown that this low energy excitonlike collective mode may be well defined at finite temperatures when the system has a strong residual s-wave pairing interaction and shows up as a distinct resonance in the Raman-scattering intensity at low-frequencies. These temperature-dependent features of Raman-scattering are specific to d-wave superconductors and hence may be of some experimental interest. This behavior is quite different from that of excitonlike modes in s-wave superconductors[12,20,21,23–25] (see also Appendix C).

Our results seem very relevant to current models of the layered cuprate superconductors. Many authors[1–4] have argued that a spin fluctuation mechanism naturally arises in the Cooper oxides, leading to Cooper pairs with $d_{x^2-y^2}$ symmetry. At the same time, there are good reasons to believe that these materials have a substantial lattice phonon-induced attractive interaction as well. In terms of the simple theoretical model we have considered, this situation is described by a pairing interaction (2), with g_0 large but still weaker than g_2. Our calculations in Sec. III show that the $\mathbf{q}=0$ excitonlike mode (see Fig. 5) has an energy which is very dependent on the magnitude of g_0 and the temperature. The lowering of the energy of this state (into a region where the quasiparticle-hole damping is weaker) leads to low-frequency Raman-scattering with a strength which increases with the temperature (see Fig. 8). In the admittedly extreme case when g_0 is only just slightly weaker than g_2, we predict a very noticeable low-energy resonance (see Figs. 9 and 10) at temperatures of order $0.75T_c$. It would be very useful to have high-resolution Raman data in this temperature and frequency region.

In our model d-wave superconductor, the excitonlike modes which correspond to excited Cooper pair states are due to the s-wave (L=0) pairing interaction g_0. However, we have seen in Sec. IV that these modes appear with substantial weight in the L=2 Raman-scattering channel. The strong effect of ordinary impurity scattering on L=2 excitonlike states in s-wave superconductors due to a d-wave pairing interaction g_2 has been carefully studied.[24,25] Analogous calculations on the effect of impurity scattering on the excitonlike state of d-wave superconductors would be useful.

We have concentrated our attention on the different behavior of the Raman spectrum of 2D d-wave superconductors due to collective effects arising from vertex corrections. Clearly our approach can also be used to calculate the effect on other physical phenomena (such as phonon self-energies.[24])

The recent work of Devereaux *et al.*[11] includes all five possible values of m in the L=2 channel for 3D d-wave superconductors, corresponding to five symmetry channels [A_{1g}, B_{1g}, B_{2g}, $E_g(1)$, and $E_g(2)$] which can be probed by Raman-scattering. In our 2D model, with pairing of B_{1g} symmetry (L=2) in conjuction with a weaker isotropic (L=0) attraction, the only Raman-scattering channel of physical interest was the B_{1g} given in (65). To complete our investigation of the Raman intensity for 2D d-wave superconductors and the role of collective modes, the inclusion of more Raman-scattering channels (A_{1g}, B_{2g}, ...) is needed in addition to the B_{1g} mode considered in Sec. IV. We note that the third paper in Ref. 11 reports gauge-invariant calculations in 2D superconductors with pairing in all d-wave channels but no s-wave pairing.

ACKNOWLEDGMENTS

We thank T. Devereaux for discussions of Raman scattering which helped clarify aspects of our work, and S. Chakravarty for a useful remark about the solution of (52). This research was supported by a grant from NSERC of Canada.

APPENDIX A: STRUCTURE OF a_ℓ, b_ℓ, c_ℓ, AND d_ℓ (ℓ=0,1,2)

We first define the following useful 2D correlation functions needed in our calculations [following CG (Ref. 9)]:

$$x_{ik\ell j}^{L,L'}(\mathbf{q},i\Omega_n)=\int\frac{d\mathbf{p}}{(2\pi)^2}f_L(\hat{\mathbf{p}})f_{L'}^*(\hat{\mathbf{p}})x_{ik\ell j}(\mathbf{p},\mathbf{q},i\Omega_n)$$
$$\equiv\overline{f_Lf_{L'}\widetilde{G}_{ik}\widetilde{G}_{\ell j}},\tag{A1}$$

where

$$x_{ik\ell j}(\mathbf{p},\mathbf{q},i\Omega_n)\equiv\frac{1}{\beta}\sum_{i\omega_m}\widetilde{G}_{ik}(\mathbf{p}+\mathbf{q},i\omega_m+i\Omega_n)$$
$$\times\widetilde{G}_{\ell j}(\mathbf{p},i\omega_m),\tag{A2}$$

and $i\Omega_n$ ($i\omega_m$) is the usual Bose (Fermi) Matsubara frequency. It is convenient to introduce

$$\widetilde{G}(\mathbf{q},i\omega_n)\equiv\tau_3\hat{G}(\mathbf{q},\omega_n),\tag{A3}$$

where the $\tau_3=\begin{pmatrix}1&0\\0&-1\end{pmatrix}$ is the Pauli-Nambu matrix. The components of this 2×2 single-particle BCS Green's function are given by

$$\widetilde{G}(\mathbf{q},i\omega_n)=\frac{\begin{pmatrix}u_{\mathbf{q}}^2&u_{\mathbf{q}}v_{\mathbf{q}}\\-u_{\mathbf{q}}v_{\mathbf{q}}&-v_{\mathbf{q}}^2\end{pmatrix}}{i\omega_n-E_{\mathbf{q}}}+\frac{\begin{pmatrix}v_{\mathbf{q}}^2&-u_{\mathbf{q}}v_{\mathbf{q}}\\u_{\mathbf{q}}v_{\mathbf{q}}&-u_{\mathbf{q}}^2\end{pmatrix}}{i\omega_n+E_{\mathbf{q}}},\tag{A4}$$

with

$$\epsilon_{\mathbf{q}}=\frac{q^2}{2m}-\mu,\quad E_{\mathbf{q}}=\sqrt{\epsilon_{\mathbf{q}}^2+|\Delta_{\mathbf{q}}|^2},$$
$$u_{\mathbf{q}}^2=\frac{1}{2}\left(1+\frac{\epsilon_{\mathbf{q}}}{E_{\mathbf{q}}}\right),\quad v_{\mathbf{q}}^2=\frac{1}{2}\left(1-\frac{\epsilon_{\mathbf{q}}}{E_{\mathbf{q}}}\right),$$
$$u_{\mathbf{q}}v_{\mathbf{q}}=\frac{\Delta_{\mathbf{q}}}{2E_{\mathbf{q}}}.\tag{A5}$$

As shown by CG, in the BCS weak-coupling limit, we only have four independent matrix elements for $x_{ik\ell j}^{L,L'}(\mathbf{p},\mathbf{q},i\Omega_n)$, namely (at T=0),

$$a(\mathbf{p},\mathbf{q},i\Omega_n)=\frac{E+E'}{2EE'}\frac{EE'-\epsilon\epsilon'}{(i\Omega_n)^2-(E+E')^2},\tag{A6}$$

$$b(\mathbf{p},\mathbf{q},i\Omega_n)=\frac{E+E'}{2EE'}\frac{-\Delta_{\mathbf{p}}\Delta_{\mathbf{p}+\mathbf{q}}}{(i\Omega_n)^2-(E+E')^2},\tag{A7}$$

$$c(\mathbf{p},\mathbf{q},i\Omega_n)=\frac{-\Delta_{\mathbf{p}}i\Omega_n}{2E}\frac{1}{(i\Omega_n)^2-(E+E')^2},\tag{A8}$$

$$d(\mathbf{p},\mathbf{q},i\Omega_n)=\frac{E+E'}{2EE'}\frac{-(EE'+\epsilon\epsilon')}{(i\Omega_n)^2-(E+E')^2},\tag{A9}$$

where $E\equiv E_{\mathbf{p}}$, $E'\equiv E_{\mathbf{p}+\mathbf{q}}$ and $\epsilon\equiv\epsilon_{\mathbf{p}}$, $\epsilon'\equiv\epsilon_{\mathbf{p}+\mathbf{q}}$. As L,L' can be 0 or 2 only, it is convenient to introduce the abbreviations $a_{00}\equiv a_0$, $a_{22}\equiv a_2$, and $a_{02}=a_{20}\equiv a_1$, etc. The latter notation is used throughout this paper.

APPENDIX B: SMALL WAVE VECTOR EXPANSION FOR a_ℓ, b_ℓ, c_ℓ, AND d_ℓ (ℓ=0,1,2)

In the long-wavelength limit ($v_Fq/\Delta\ll1$), one can expand the various correlation functions given in Appendix A,

$$x_\ell(\mathbf{q},\omega) \equiv x_\ell(q,\omega) = x_\ell(\omega) + \frac{1}{2}\frac{v_F^2 q^2}{\Delta^2} N(0) x_\ell''(\omega) + O\left(\frac{v_F^4 q^4}{\Delta^4}\right), \quad \text{(B1)}$$

where the 2D density of states is $N(0) = m/\pi$ and the odd-order terms in q make no contribution as a result of the Fermi surface average. The above expansion assumes the gap is slowly varying near the Fermi surface, i.e., $\Delta_{\mathbf{p}+\mathbf{q}} \simeq \Delta_{\mathbf{p}}$. Here $x_\ell(\omega) \equiv x_\ell(\mathbf{q}=0,\omega)$ and we have defined

$$x_\ell''(\omega) \equiv \frac{\Delta^2}{v_F^2 N(0)} \left.\frac{d^2 x_\ell(q,\omega)}{dq^2}\right|_{q=0}. \quad \text{(B2)}$$

The nonvanishing zeroth-order terms $x_\ell(\omega)$ in (B1) are given by

$$\begin{aligned}
a_0(\omega) &= -b_0(\omega) = -N(0)I_2(\bar\omega),\\
d_0(\omega) &= -\frac{1}{\bar g_2} + 4\bar\omega^2 N(0) I_0(\bar\omega) - N(0)I_2(\bar\omega),\\
c_1(\omega) &= \sqrt{2}\bar\omega N(0) I_2(\bar\omega),\\
a_2(\omega) &= -b_2(\omega) = -N(0)I_4(\bar\omega),\\
d_2(\omega) &= -\frac{1}{g_2} + 4\bar\omega^2 N(0) I_2(\bar\omega) - N(0)I_4(\bar\omega),
\end{aligned} \quad \text{(B3)}$$

where the functions $I_i(\bar\omega)$ are defined by [$f_2(\hat{\mathbf{p}})$ is real]

$$I_i(\bar\omega) \equiv -\frac{1}{16}\int_{-\infty}^{\infty} d\bar\epsilon \int_0^{2\pi} \frac{d\phi'}{2\pi} \frac{f_2^i(\hat{\mathbf{p}})}{\bar E(\bar\omega^2 - \bar E^2)}. \quad \text{(B4)}$$

The scaled energies are $\bar\omega = \omega/2\Delta$, $\bar\epsilon \equiv \epsilon/\Delta$, and $\bar E \equiv E/\Delta$. The parameter $\bar g_2$ in d_0 in (B3) is defined by

$$-\frac{1}{\bar g_2} \equiv \sum_{\mathbf{p}}^{\omega_c} \frac{1}{2E_{\mathbf{p}}}, \quad \text{(B5)}$$

where ω_c is the usual BCS frequency cutoff in the pairing interaction. Using the d-wave gap equation[14]

$$-\frac{1}{g_2} = \sum_{\mathbf{p}}^{\omega_c} \frac{|f_2(\hat{\mathbf{p}})|^2}{2E_{\mathbf{p}}}, \quad \text{(B6)}$$

one can show that $\bar g_2 = g_2$. We recall that $f_2^2(\hat{\mathbf{p}}) = 1 + \cos(4\phi)$, and the term $\cos(4\phi)$ makes no contribution to the rhs of (B6).

The second-order terms in (B1) are obtained after some lengthy algebra:

$$\begin{aligned}
a_0''(\omega) &= J_{231}(\bar\omega) - \frac{3}{8}J_{451}(\bar\omega) - J_{212}(\bar\omega) + \frac{3}{2}J_{432}(\bar\omega) + 16 J_{2-13}(\bar\omega) - 8J_{413}(\bar\omega),\\
b_0''(\omega) &= -a_0''(\omega) + \frac{1}{2}J_{231}(\bar\omega),\\
c_0''(\omega) &= -\sqrt{2}\bar\omega\left[J_{112}(\bar\omega) + \frac{1}{2}J_{332}(\bar\omega) + 16J_{1-13}(\bar\omega) - 8J_{313}(\bar\omega)\right],\\
d_0''(\omega) &= a_0''(\omega) + J_{011}(\bar\omega) + 8J_{0-12}(\bar\omega) - 4J_{212}(\bar\omega) - 4\bar\omega^2\left[J_{012}(\bar\omega) + \frac{1}{2}J_{232}(\bar\omega) + 16J_{0-13}(\bar\omega) - 8J_{213}(\bar\omega)\right].
\end{aligned} \quad \text{(B7)}$$

The new functions $J_{ijk}(\bar\omega)$ are defined as

$$J_{ijk}(\bar\omega) \equiv \frac{1}{8}\int_{-\infty}^{\infty} d\bar\epsilon \int_0^{2\pi} \frac{d\phi'}{2\pi} \frac{f_2^i(\hat{\mathbf{p}})\cos^2(\phi-\phi')}{\bar E^j(\bar\omega^2 - \bar E^2)^k}, \quad \text{(B8)}$$

where ϕ is the angle of $\mathbf{q}$ (Fig. 1). The functions $x_1''(\omega)$ and $x_2''(\omega)$ ($x = a, b, c, d$) have an identical form to $x_0''(\omega)$ in (B7), except that for $x_1''(\omega)$ we replace J_{ijk} by J_{i+1jk} in $x_0''(\omega)$, and for $x_2''(\omega)$ we replace J_{ijk} by J_{i+2jk} in $x_0''(\omega)$.

These long-wavelength approximations for the noninteracting correlation functions in Appendix A are valid at all frequencies. One may make further simplifying approximations when discussing different frequency regions (ω as compared to 2Δ).

APPENDIX C: EXCITONLIKE MODES IN s-WAVE SUPERCONDUCTORS

For comparison, we briefly review the excitonlike modes (L=2) and the associated Raman-scattering intensity for a 2D s-wave superconductor.[12,20] One may easily verify that the L-channel collective mode will be given by the zeros of [see (19) for $\Delta_{\mathbf{p}} = \Delta$ and again, $N(0)g_0 \to g_0$ and $N(0)g_2 \to g_2$]

$$D_L^s \equiv [1 + (g_L - 2v_{\mathbf{q}}\delta_{0,L})A_L](1 + g_L B_L) + 4g_L(g_L - 2v_{\mathbf{q}}\delta_{0,L})c_L^2, \quad \text{(C1)}$$

where s denotes an s-wave superconductor and the functions A_L, B_L, and c_L ($L = 0, 2$) follow the notation used in Sec. II for d-wave superconductors (see also Appendix A). The collective mode in the L=0 channel is the AB phonon mode. This is renormalized into a 2D plasmon by the Coulomb interaction and has no weight in the Raman-scattering intensity. The Coulomb interaction has no effect in the L=2 channel. We note that while the pairing interaction g_0 does not appear explicitly in (C1) for L=2, it enters implicitly through the gap parameter. For $\mathbf{q} = 0$ and T=0, we obtain the analytic form for (C1) in the L=2 channel [compare with (45)–(48)],

$$D_2^s(\omega) = \left[1 - \frac{1}{4}g_2 I(\bar\omega)\right]\left[1 - \frac{g_2}{g_0} + \frac{1}{4}g_2\bar\omega^2 I(\bar\omega)\right] + \frac{1}{16}g_2^2\bar\omega^2 I^2(\bar\omega), \tag{C2}$$

where we have introduced the functions

$$I(\bar\omega) = \begin{cases} \frac{2}{\bar\omega\sqrt{1-\bar\omega^2}}\arcsin\bar\omega, & \bar\omega < 1, \\ \frac{2}{\bar\omega\sqrt{\bar\omega^2-1}}[\ln(\bar\omega - \sqrt{\bar\omega^2-1}) + i\frac{\pi}{2}], & \bar\omega > 1\,. \end{cases} \tag{C3}$$

One can see from (C3) that the imaginary part of the function $I(\bar\omega)$ only contributes when $\omega \geq 2\Delta$; i.e., there is no pair breaking region below 2Δ.

We can rewrite (C2) as

$$D_2^s(\omega) = [1 - g_2 R_+(g_0,\bar\omega)][1 - g_2 R_-(g_0,\bar\omega)], \tag{C4}$$

where the functions $R_\pm$ are defined by

$$R_\pm(g_0,\bar\omega) = \frac{1}{2}\left(\frac{1}{g_0} + \frac{1}{4}I(\bar\omega)(1-\bar\omega^2)\right) \mp \frac{1}{2}\left[\left(\frac{1}{g_0} + \frac{1}{4}I(\bar\omega)(1-\bar\omega^2)\right)^2 - \frac{1}{g_0}I(\bar\omega)\right]^{\frac{1}{2}}. \tag{C5}$$

Using (C4), the collective modes are given by the solutions of

$$\frac{1}{g_2} = \mathrm{Re}R_-(g_0,\bar\omega) \tag{C6}$$

for $g_2 < 0$; these correspond to "particle-particle"-type excitonlike modes. For comparison with *d*-wave superconductors (see Fig. 5), we illustrate the solution of (C6) in Fig. 11. When $|g_2| > |g_0|$, the corresponding solution

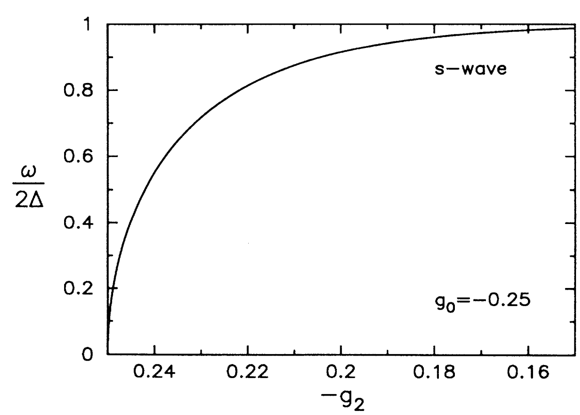

FIG. 11. The frequency of the excitonlike mode in a 2D *s*-wave superconductor ($\mathbf{q} = 0$, T=0) vs the magnitude of the attractive L=2 interaction g_2. Compare with Fig. 5.

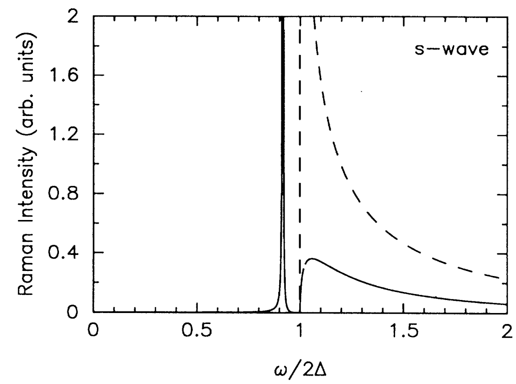

FIG. 12. The frequency dependence of the T=0 Raman-scattering intensity for a 2D *s*-wave superconductor in the L=2 channel, for fixed $g_0 = -0.25$, $g_2 = -0.20$ (solid line) and $g_0 = -0.25$, $g_2 = -0.01$ (dashed line). A bound state below the continuum 2Δ is visible when g_2 is large enough. The curves are convoluted with a resolution function of width $\Gamma = 0.01$ (see Ref. 20 for analogous results for 3D superconductors).

is found to correspond to an imaginary frequency, which indicates the expected instability of the system with a *s*-wave pairing order parameter in this case.

The L=2 Raman-scattering intensity is given by [compare with (66) and (67)]

$$\widetilde{S}_s^{L=2}(\bar\omega) = \mathrm{Im}\left[\frac{R_2^s(\omega)}{1 + g_2 R_2^s(\omega)}\right], \tag{C7}$$

where

$$R_2^s(\omega) = -\frac{1}{4}I(\bar\omega) + \frac{\frac{1}{16}g_2\bar\omega^2 I^2(\bar\omega)}{1 + g_2[-1/g_0 + \frac{1}{4}\bar\omega^2 I(\bar\omega)]}. \tag{C8}$$

The frequency dependence of the L=2 Raman-scattering intensity for a 2D *s*-wave superconductor given by (C7) is plotted in Fig. 12, for $g_2 = -0.20$ and -0.01, with a fixed value of $g_0 = -0.25$ (see also Fig. 1 in Ref. 20). When $g_2 \to 0$, we have $R_2^s(\omega) \propto I(\bar\omega)$ and thus $\widetilde{S}_s^L(\bar\omega) \propto \mathrm{Im}I(\bar\omega)$. This Raman spectrum exhibits a square-root singularity at $\omega = 2\Delta$, which corresponds to the two-particle spectrum in the absence of vertex corrections. In contrast, when g_2 is finite (as discussed at length in Ref. 20 for 3D superconductors), the L=2 Raman-scattering spectrum for *s*-wave superconductors consists of a sharp peak at $\omega < 2\Delta$ corresponding to a well-defined excitonlike mode (see Fig. 11) and a continuum with a broad maximum for $\omega > 2\Delta$. Unfortunately, in the usual *s*-wave superconductors, there is no reason to believe that an attraction in the *d*-wave channel will be very strong and thus any excitonlike mode will always have an energy very close to the *p*-*h* continuum at 2Δ.[12,24]

[1] P. Monthoux, A. V. Balatsky, and D. Pines, Phys. Rev. Lett. **67**, 3448 (1991); Phys. Rev. B **46**, 14803 (1992).
[2] N. Bulut and D. J. Scalapino, Phys. Rev. Lett. **68**, 706 (1992).
[3] P. Monthoux and D. Pines, Phys. Rev. Lett. **69**, 961 (1992); Phys. Rev. B **47**, 6069 (1993).
[4] D. Thelen, D. Pines, and J. P. Lu, Phys. Rev. B **47**, 9151 (1993).
[5] Z.-X. Shen *et al.*, Phys. Rev. Lett. **70**, 1553 (1993).
[6] W. N. Hardy, D. A. Bonn, D. C. Morgan, R. Liang, and K. Zhang, Phys. Rev. Lett. **70**, 3999 (1993).
[7] D. A. Wollman, D. J. Van Harlingen, W. C. Lee, D. M. Ginsberg, and A. J. Leggett, Phys. Rev. Lett. **71**, 2134 (1993).
[8] For a useful summary, see B. G. Levi, Phys. Today **46**(5), 17 (1993).
[9] R. Côté and A. Griffin, Phy. Rev. B **48**, 10404 (1993).
[10] D. S. Hirashima and H. Namaizawa, J. Low Temp. Phys. **73**, 137 (1988).
[11] T. P. Devereaux, D. Einzel, B. Stadlober, D. H. Leach, and J. J. Neumeier, Phys. Rev. Lett. **72**, 396 (1994); T. P. Devereaux and D. Einzel, Physica B **194-196**, 1531 (1994); T. P. Devereaux, D. Einzel, B. Stadlober, and R. Hackl, Phys. Rev. Lett. **72**, 3291 (1994).
[12] A. Bardasis and J. R. Schrieffer, Phys. Rev. **121**, 1090 (1961).
[13] P. W. Anderson and P. Morel, Phys. Rev. **123**, 1911(1961).
[14] The temperature dependence of $\Delta(T)/\Delta(0)$ in planar d-wave superconductors is given by H. Won and K. Maki, Phys. Rev. B **49**, 1397 (1994). These authors also evaluate various thermodynamic and transport coefficients (at zero frequency), ignoring vertex corrections.
[15] P. W. Anderson, Phys. Rev. **112**, 1900 (1958).
[16] P. C. Martin, in *Superconductivity*, edited by R. D. Parks (Dekker, New York, 1969), Vol. 1, p. 371.
[17] H. A. Fertig and S. Das Sarma, Phys. Rev. B **44**, 4480 (1991).
[18] L. Belkhir and M. Randeria, Phys. Rev. B **49**, 6829 (1994).
[19] P. B. Littlewood and C. M. Varma, Phys. Rev. B **26**, 8798 (1982).
[20] H. Monien and A. Zawadowski, Phys. Rev. B **41**, 8798 (1990).
[21] I. Tüttő and A. Zawadowski, Phys. Rev. B **45**, 4842 (1992).
[22] This approach for dealing with Cooper pair fluctuations was developed by C. Caroli and K. Maki, Phys. Rev. **159**, 306 (1967), to treat type-II s-wave superconductors. The method was first used by L. P. Kadanoff and I. I. Falko, Phys. Rev. **136**, A1170 (1964).
[23] M. V. Klein and S. B. Dierker, Phys. Rev. B **29**, 4976 (1984).
[24] T. P. Devereaux, Phys. Rev. B **45**, 12965 (1992); **47**, 5230 (1993).
[25] K. Maki and T. Tsuneto, Prog. Theor. Phys. (Kyoto) **28**, 163 (1962).